Simulated decline of a northern forest due to anthropogenic controls on the regeneration-mortality balance

Adam Erickson[1,†*], Craig Nitschke[2], and Gordon Stenhouse[3]

[1]Integrated Remote Sensing Studio, Department of Forest Resources Management, University of British Columbia, 2045-2424 Main Mall, Vancouver, British Columbia, V6T 1Z4, Canada

[2]School of Ecosystem and Forest Sciences, University of Melbourne, 500 Yarra Boulevard, Richmond, Victoria, 3121, Australia

[3]Foothills Research Institute, Box 6330, Hinton, Alberta, T7V 1X6, Canada

[†]*Current address*: Hydrological Sciences Laboratory, Code 617, NASA Goddard Space Flight Center, Greenbelt, Maryland, 20771, USA

[*]Corresponding author: adam.michael.erickson@gmail.com

ORCID: 0000-0002-8730-073X

Twitter: @admercs

Non-peer-reviewed pre-print submitted to EarthArXiv

Keywords: forest model; tree regeneration; forest resilience; anthropogenic; wildfire; boreal

Abstract

The population structure of forests is shaped by balancing the opposing forces of regeneration and mortality, each of which influence C turnover rates and are sensitive to climate. Regeneration underlies the migrational potential of forests to climatic change and remains underserved in modeling studies. Our objective was to test the hypothesis that warming may reduce tree regeneration rates while amplifying fire regimes, producing forest loss. Absent sites within dispersal limits, trees may fail to track the velocity of warming, producing a decline in forested area. Long-term implications include changes to biogeochemical and energetic balances, species composition, and evolutionary trajectories. We performed hybrid model simulations to assess the resilience of forests to past-century conditions over the next fifty years in western Canada. We conducted simulations at a species-level taxonomic resolution to capture genotypic/phenotypic variability in response to climate. A recent shift toward small, frequent, human-caused fires and warming-reduced regeneration diminished species migration potential. The simulated rate of forest migration lagged behind temperature equilibria by 319 m yr-1. Understanding species migrational potential is particularly critical for northern forests, which have warmed at a rate twice the global mean. Our findings highlight the effect of diminished regeneration due to climatic change, a process neglected in current global-scale terrestrial biosphere models used in climate studies. We suggest that future terrestrial biosphere model studies incorporate these demographic rates in their findings on global change, as they carry substantial climatic and evolutionary implications.

Introduction

Seasonal fire and climate cycles played a central role in the evolution of boreal forests. Here, large stand-replacing fires have been the dominant disturbance type for millennia (Rowe and Scotter 1973; Davis and Shaw 2001; Rogers et al. 2015), while temperatures historically reached cold extremes. In North America, boreal tree species evolved a diversity of adaptations to fire, including vegetative resprouting, cone serotiny, aerial seed banks, fire-enhanced regeneration, and increased flammability (Schwilk and Ackerly 2001; Keeley et al. 2014; Pounden et al. 2014; Rogers et al. 2015). These adaptations are believed to impart trees with a competitive advantage in the successional phases of disturbance and regeneration.

Trees in the Canadian boreal exhibit a high degree of intraspecific genetic variation and local adaptation (Davis and Shaw 2001). Trees respond to periodic climatic cycles *in situ* via phenotype plasticity (i.e., gene expression) and to long-term climatic change through emigration (Aitken et al. 2008; Matzke and Mosher 2014). Extreme events beyond physiological tolerances produce damage or mortality. While the distribution of tree species correlates well with historical climate at coarse spatiotemporal scales, disturbance responses dominate fine-scale patterns (Prentice 1986). Trees often lag behind climatic optima (Bertrand et al. 2011), requiring a semi-sequential process of mortality, reproduction, dispersal, and regeneration to transition forest composition toward optimality.

When the land velocity of temperature or moisture changes outpace the availability of sites for recruitment given disturbance patterns and dispersal rates (Clark et al. 1998), climatic change may occur too rapidly for tree migration to track warming. Given a failure to migrate, *in situ* regeneration conditions can become increasingly suboptimal (Nitschke and Innes 2008). When multiple species fail to track warming, absent new migrants, forest decline can occur, which may explain recently observed reduced forest cover for the greater Rocky Mountain region (Hogg et al. 2008; van Mantgem et al. 2009; Allen et al. 2010; Michaelian et al. 2011; Mascaro et al. 2011; Martínez-Vilalta et al. 2012; Vilà-Cabrera et al. 2013; Worrall et al. 2013; Cohen et al. 2016). Over longer timescales, gradual forest decline may give way to compositional or landcover change. Reduced mortality rates (e.g., due to increased fire suppression) may inhibit compositional changes, obfuscating latent migration processes underway. This may result in more pronounced compositional changes when disturbance rates recover to pre-suppression levels.

Due to the accelerated pace of high-latitude warming, boreal climatic conditions are shifting northward at a rate of 430 m yr^{-1} (Loarie et al. 2009; Hamann et al. 2015). The rate of recent warming surpasses observed Quaternary rates of species range shifts inferred from the pollen record (Davis and Shaw 2001), while landscape fragmentation may pose a further constraint on climatic optimality (Lazarus and McGill 2014). While direct measurements of species migrations and other forest dynamics remain limited by the large spatiotemporal scales of the processes involved, simulation models provide a useful tool for discerning likely historical and future patterns. The combination of simulation models and adaptive management (Holling 1978) may eventually facilitate ecological optimization of management goals, such as maximizing carbon storage, structural heterogeneity, or tree species diversity.

Here, forest compositional and structural changes given past-century climate and fire trends are simulated for 50 years in the Alberta study area, beginning at year 2000 conditions. This was done to infer the resilience of contemporary forests given the persistence of past-century climate and fire patterns. We focus on recent observations rather than future climate and fire projections to minimize the uncertainty regarding the likelihood of the simulated conditions by utilizing well-described historical periods. Our hybrid forest landscape model was initialized at year 2000 conditions using modeled tree species distributions (Gray and Hamann 2012) classified into Canadian landcover classes, given the high quality of data available for this period. Four historical joint climate-fire-anthropogenic periods were used to simulate past-century forest successional trajectories. Differences in stand conditions were assessed after 50 years of simulation, with the initial ten years used for model spin-up. By simulating these four historical scenarios, we assess the resilience of extant forests to the persistence of past-century climate, fire, and anthropogenic trends.

Material and methods

We combined the Tree and Climate Assessment Establishment Model, TACA-EM (Nitschke and Innes 2008), within the second LANdscape DIsturbance and Succession model, LANDIS-II (Scheller et al. 2007), to simulate forest dynamics across a 25.2 Mha landscape in the southern Canadian Rocky Mountain region at one-hectare resolution. While the western Alberta study area is comprised of 25.2 M one-ha cells, 71% or 18 M cells are active (containing natural vegetation), after masking out developed land, waterbodies, and bare rock (Figure 1). The study area represents an elevational and latitudinal gradient between boreal, montane Cordilleran forests, and prairie. Here, differences in elevation-related climatic and edaphic patterns are believed to control vegetation species assemblages though disturbances and soil moisture effects (White and Mathewes 1986; Hogg 1994; Moss 2012). Using the Natural Regions and Subregions of Alberta (Natural Regions Committee 2006), the majority of the study area is located in the Boreal region (46.2% of the study area), followed by the Foothills (25.5%) and Rocky Mountain (19.5%) regions. The Parkland and Grassland regions together comprise less than 10% of the study area, making over 90% of the study area boreal and montane, characterized by a strong east-west elevational gradient (Erickson et al. 2015).

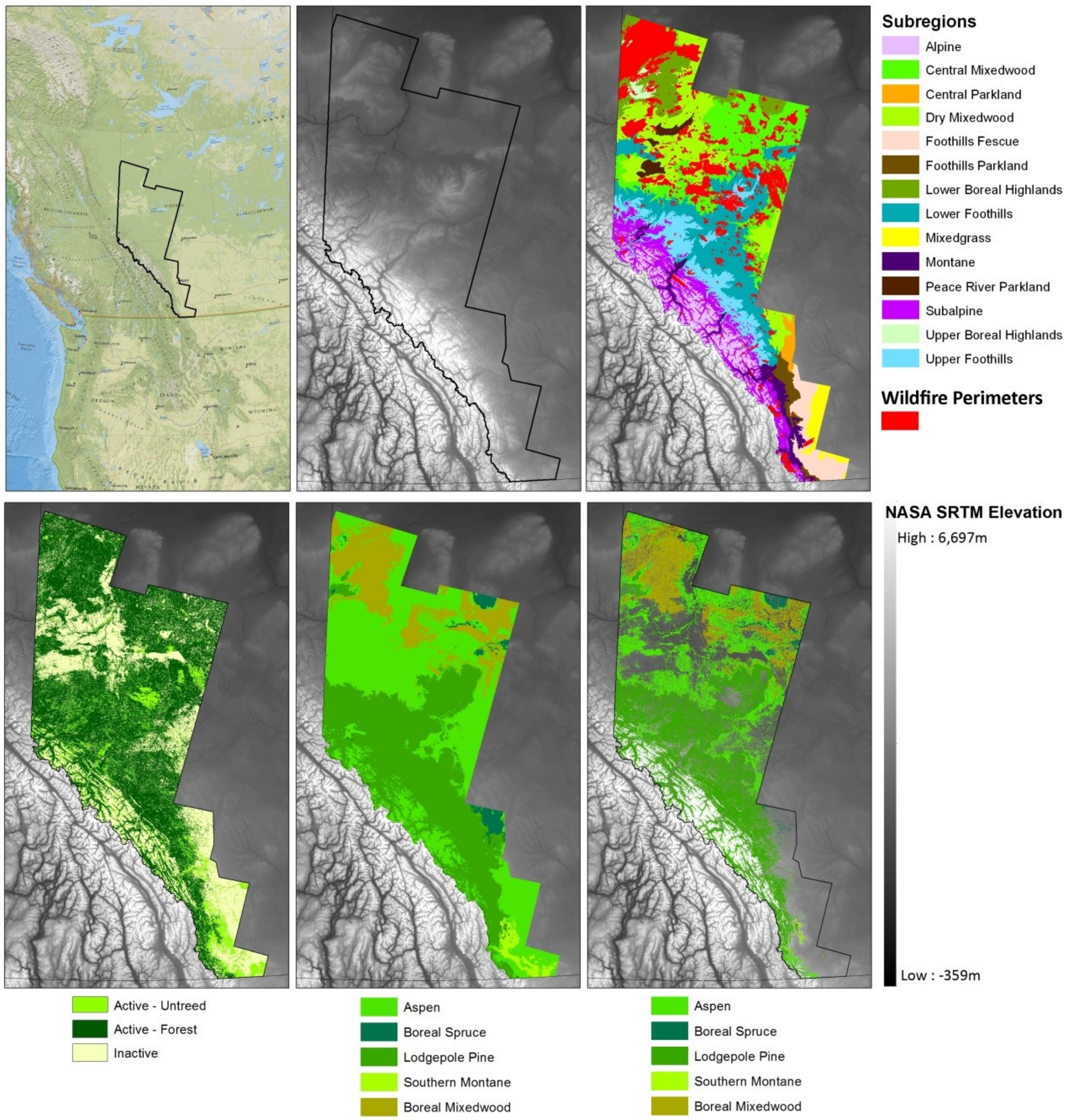

Figure 1. Study area, historical wildfire perimeters, biogeoclimatic subregions, and landscape initialization process: (top-left) regional context; (top-middle) NASA SRTM topography (meters); (top-right) historical wildfire perimeters overlaid on biogeoclimatic subregions; (bottom-left) inactive (static) sites and active (dynamic) sites with and without trees; (bottom-

middle) rules-based forest composition classification; (bottom-right) forest composition classes with inactive sites masked from the landscape initialization; all raster data used in the model was resampled to 100-meter resolution and co-registered.

The TACA-EM and LANDIS-II models and their parameterization are detailed in the supplementary materials. Both models previously underwent validation and sensitivity analysis in North America (Mladenoff et al. 1993; Scheller and Mladenoff 2004; Scheller et al. 2007; Nitschke and Innes 2008; Nitschke et al. 2008, 2012; Simons-Legaard et al. 2015). Within LANDIS-II, two types of wildfire models were applied: (1) a simple statistical fire-spread model; (2) a semi-mechanistic cost-path fire-spread model incorporating fire weather inputs and landcover change to dynamically update site fuel conditions. The semi-mechanistic fire model was developed from forest fire data in Canada (Wagner 1977; Van Wagner 1987, 1989; Forestry Canada Fire Danger Group 1992). For each fire model, a stochastic optimization algorithm based on stochastic gradient descent (Widrow and Hoff 1960) was applied for parameter tuning, overcoming a long-standing practical limitation to large-scale simulations (He and Mladenoff 1999). The overall simulation framework is shown in the supplementary materials (Figure S1).

TACA-EM was run separately for each of the climate scenarios and biogeoclimatic regions similar to previous research (Erickson et al. 2015). The resultant tree species establishment probabilities were fed into LANDIS-II together with the other parameters for each scenario. Simulations were run for 50 years at annual resolution, with the first 10 years used for model spin-up. Model spin-up was used to produce empirical disturbance-driven age class patterns given the importance of fire in shaping these patterns (Boychuk and Perera 1997). The LANDIS-II model was initially run at 500 m resolution to accelerate convergence of parameter optimization using stochastic gradient descent (Widrow and Hoff 1960), or SGD, a variant of the steepest descent method (shown in yellow in Figure S1). In SGD, parameter values are updated in the direction and magnitude, or generally, gradient ∇ of reduced model error, iteratively updated with stochasticity based on previous simulations. The SGD algorithm relies on principles common to iterative gradient-based optimization methods (Supplementary materials).

In this work, we utilized the inherently stochastic nature of the LANDIS-II model to provide stochastic updates, while the gradient direction $\vec{p}_i$ and step width l_i were calculated by hand after each simulation iteration. The SGD optimization method is widely used alongside the backpropagation algorithm (Dreyfus 1962; Linnainmaa 1970) in deep learning for training artificial neural networks (LeCun et al. 2015). Final model optimization runs were conducted at 100 m resolution to balance computational cost and the grain size needed to capture the effects of fine-scale disturbance patterns, approaching the resolution limits of the LANDIS-II model.

Historical fire regimes

Regional fire regime parameters were derived from the Canadian National Fire Database (NFDB) spatial wildfire data. The NFDB database was produced from an analysis of airborne and satellite imagery together with field plot data. Fire rotation period (FRP), or fire cycle, is one of the most commonly applied metrics to indicate the severity of fire regimes, with lower values indicating greater severity. FRP is typically calculated alongside the mean fire return interval (MFRI), or average time between fires for a given area or individual site – an indicator of fire frequency. FRP is the mean time required for the sum of fire sizes within an area to equal that area in size, calculated over a given time interval. Hence, FRP is the area-normalized MFRI. Applied to individual sites, FRP is simply equal to MFRI. By normalizing for area, FRP provides more information about fire regimes at scales greater than the individual site without requiring additional data collection. MFRI values calculated for areas of different sizes are not directly comparable, unless normalized for area, which produces FRP values. Accordingly, we focus on FRP in our historical fire regime analysis. While other changes in the distribution of fires provide added information, FRP provides a single robust indicator of fire regimes. Calculations for FRP and MFRI are given below.

FRP = Time Interval / (Sum of Fire Sizes or Sites Burned in Area / Area Size)

MFRI = Time Interval / Number of Fires in Site or Area

Model scenarios

Fourteen 50-year simulations were run at an annual resolution, corresponding to four historical periods, three model configurations, and two extremes scenarios, to determine forest resilience under the persistence of past-century climate and fire trends with year 2000 initial conditions. A 50-year simulation duration was selected for its relevance to management timescales and to balance initial conditions and model behavior (e.g., equilibrium at 500-year timescales), as error propagates over time in simulations, increasing uncertainty. Historical climate and fire conditions were classified into the following three 30-year periods: Pre-Suppression Era (1923-1952), Early Suppression Era (1953-1982), and Global Change Era (1983-2012), corresponding to changes in fire suppression, climate, and human activity. A Most Recent Decade (2003-2012) scenario was included to encapsulate current regimes, based on an observed inflection point in fire frequency and size.

With the exception of the Extremes scenarios, each of the four scenarios was run under three different model configurations: (1) Succession only (*ao*); (2) Succession with Base Fire (*ao-bf*); (3) Succession with Dynamic Fire (*ao-dffs*). This was done to control for the effects of climate and fire on forest structural and compositional change. For the two Extremes scenarios, Pre-Suppression Era fire regimes – the most severe burn rate – were applied to Most Recent Decade climatic conditions – the warmest conditions – to determine the relative contributions of climate and fire on forest compositional and structural change in the most extreme cases. The simulation scenarios (configuration and period combinations) are abbreviated as shown in the supplementary information (Table S1).

For each scenario, spatiotemporal metrics indicative of directional change at the landscape scale were tracked, including latitudinal and elevational variation in species regeneration and relative abundance, as well as changes to forest structure (inferred from site age classes) and area. A focus on climate and fire is intended to represent changes to the two primary controls on boreal forest dynamics.

Results

Three-fold decline in fire rotation period despite warming

Fire rotation period (FRP) increased by 298% between the 30-year Pre-Suppression (1923-1952) and Global Change (1983-2012) periods, indicating an approximate three-fold reduction in fire regime severity during a period of known warming. FRP increased by 166% between the Pre-Suppression and Early Suppression (1953-1982) periods, before increasing by another 50% between the Early Suppression and Global Change periods. FRP was effectively unchanged between the Global Change and Most Recent Decade (2003-2012) periods, deviating by -0.1% compared to the 30-year mean. However, Most Recent Decade fires were nearly twice as frequent at half the mean fire size (MFRI Δ = -45%; annual frequency Δ = +82%; MFS Δ = -43.3%).

Adjusted for area, across all periods, the Boreal region had the shortest fire rotation period (FRP), followed by the Foothills and Rocky Mountain regions. The lower-elevation Parkland region had the longest FRP, followed by the Grassland region. The Boreal shows the greatest area burned and, by a lower margin, greatest proportion of the study area. FRP increased across the three periods, indicative of diminished burning. Between the Pre-suppression and Global Change Eras, FRP lengthened the most in the Boreal and Foothills regions while declining the most in the Parkland and Rocky Mountain regions. An analysis at the finer scale shows an acute increase in the FRP for the Peace River Parkland and Dry Mixedwood subregions, while the Upper Foothills subregion declined. All higher elevation subregions showed intensifying burning indicative of warming (Supplementary material, Figure S2).

Our stochastic gradient descent-based optimization algorithm markedly improved fire model calibration ($\overline{R^2}$= 0.96; $\overline{\Delta R^2}$ = +0.14), yielding simulation results closely matching observations from the Canadian National Fire Database. Based on a visual analysis of simulation results for maximum cohort age classes resulting from fire region parameterizations, the boreal region exhibited the greatest fire-related structural (i.e., mean and standard deviation of site age class) change across scenarios. Frequent large fires during the Pre-Suppression Era produced a homogeneous structural patchwork of forests, while frequent small fires in the two most recent scenarios produced a diffuse forest landscape age pattern and decline in area burned, corresponding to observed empirical changes.

While base fire better fit aggregate 30-year statistics for observed fire regimes, time-series comparisons between simulated and observed regimes showed that dynamic fire better captured the mean and variability for both annual fire frequency and area burned. Wavelet spectra for annual 1-D time-series showed higher and lower wavelet dissimilarity (Rouyer et al., 2008) for dynamic fire area burned and fire frequency, respectively, compared to base fire (Supplementary material, Table S5). Wavelet spectra decompose the variance of 1-D time-series over a 2-D time-frequency plane and can be used to analyze the covariance of non-stationary signals with noise (Rouyer et al., 2008).

In the dynamic fire model results, iteratively updated landscape fuel conditions, based on 2012-2013 fire weather, reduced fire frequency and area burned in each scenario compared to base fire. For the most severe fires, in the Pre-Suppression Era, base fire model results showed large fires during the initial simulation year and relatively flat activity until simulation year ~ 45. The temporal distribution of fire frequency was more stable and realistic in the dynamic fire scenarios due to the fuel-limited semi-mechanistic model design, while base fire exhibited brute-force application of statistical model parameters (Figure 2).

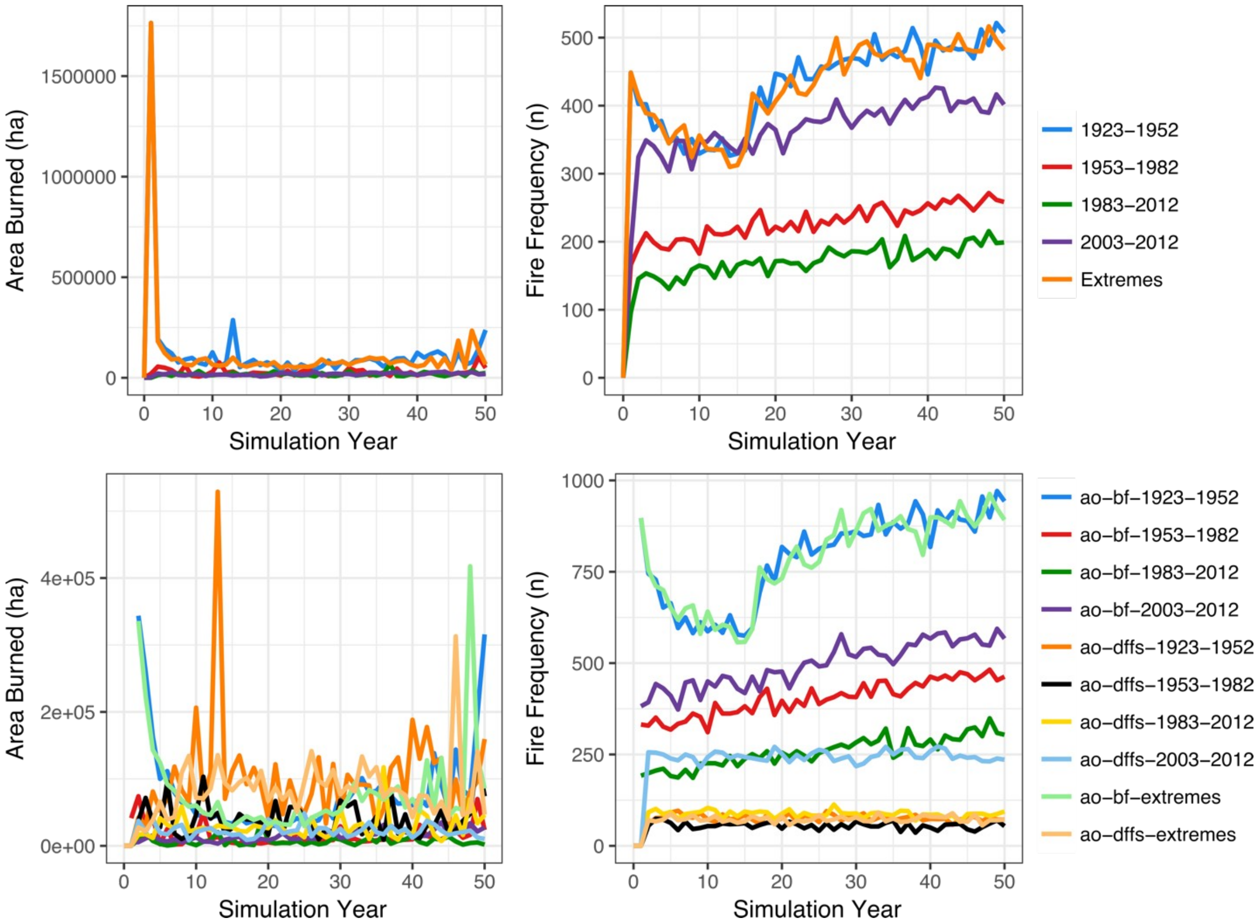

Figure 2. Simulated annual fire regimes by period (top) and scenario (bottom): (top-left) annual simulated area burned by period; (top-right) annual simulated fire frequency by period; (bottom-left) annual simulated area burned by scenario; (bottom-right) annual simulated fire frequency by scenario; refer to Table S1 for scenario codes

Reduced regeneration potential under warming

TACA-EM model results indicate that conditions for tree regeneration were increasingly suboptimal, declining across the 1923-2012 study period (Figure 3). Optimal regeneration conditions occurred most frequently in the Rocky Mountain, Parkland, and Foothills regions. The Boreal region remained the most stable, while Montane regions maintained higher overall regeneration potential. An increased frequency and depth of modeled drought, due to changes to soil water balance, most limited regeneration conditions in the Grassland region, where fluvial and aeolian soils are abundant. These results were critical to changes observed in LANDIS-II simulations, due to interactions between mortality and regeneration.

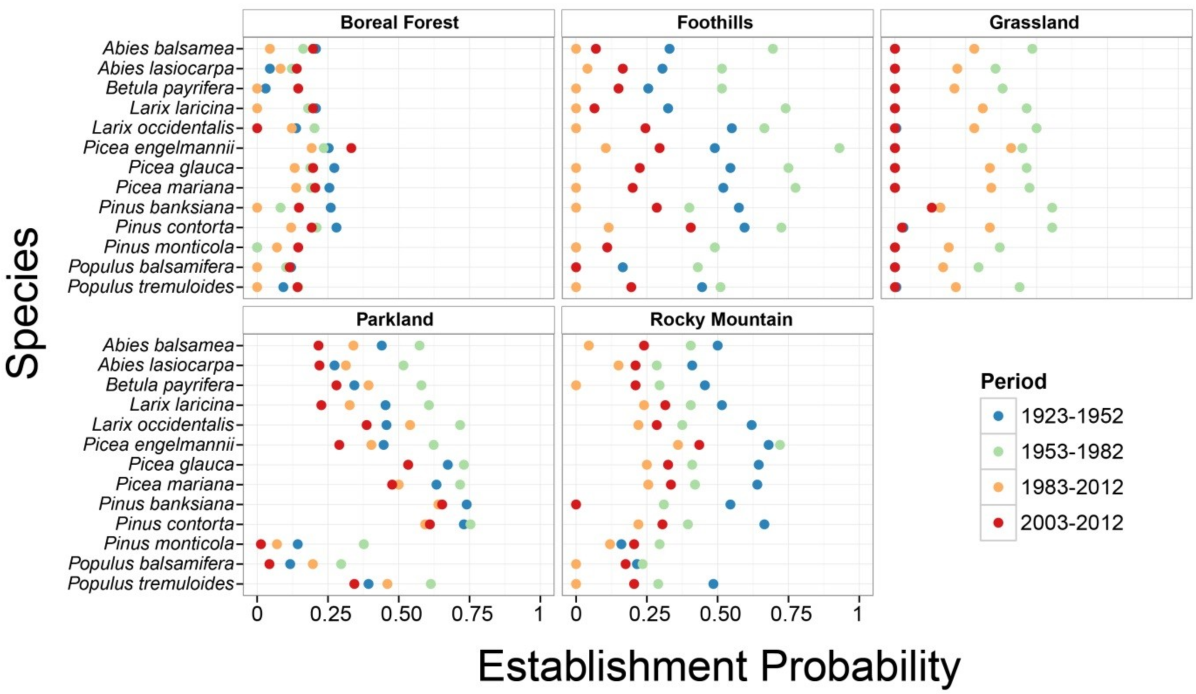

Figure 3. Probability of tree species regeneration for thirteen subregions within five biogeoclimatic regions, 1923 to 2012: blue = 1923-1952; green = 1953-1982; orange = 1983-2012; red = 2003-2012

LANDIS-II model results showed a decline in forested area for the most severe fire scenarios and an increase in forested area for mild disturbance scenarios. Forest decline indicates a failure to regenerate post-disturbance and/or an annual rate of burning outpacing the rate of regeneration. Resprouting and serotinous species regenerate post-fire each simulation year, the latter requiring that seed availability and establishment conditions be met. An initial rapid increase in forested area for most scenarios is attributable to recruitment into sites classified as open (i.e., untreed active cells) in the initial landscape. The maximum total forested area was 38% greater than the minimum area, resulting from differences in fire regime severity and regeneration suitability. For the Pre-Suppression Era and Extremes scenarios, base fire produced the largest disturbances and thus the greatest change in forested area. While greater fire disturbances removed more species-age cohorts, warming climatic conditions reduced post-fire regeneration, further diminishing the forested area (Figure 4).

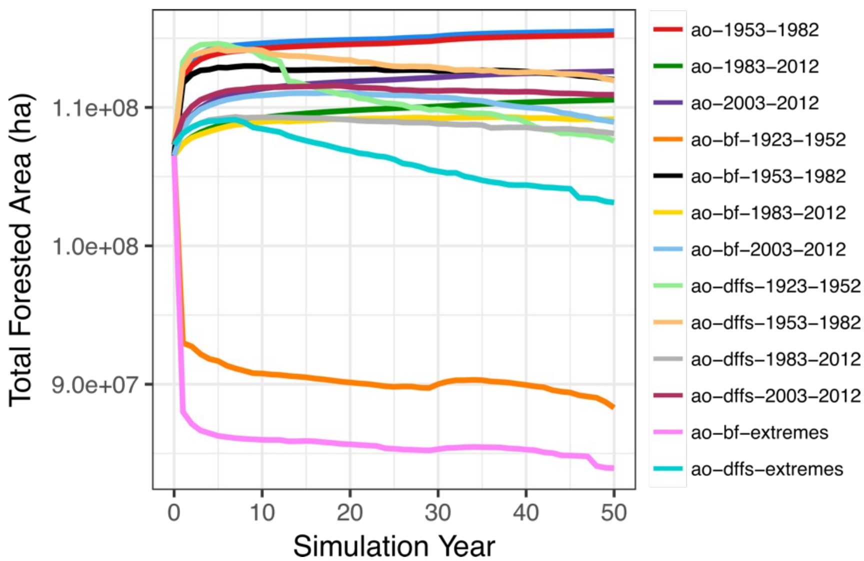

Figure 4. Annual total forested area (number of 1-ha pixels) by year and scenario; includes forests of all age classes; refer to Table S1 for scenario codes

While warming reduced the likelihood of regeneration over the simulation period, variation in fire regimes produced more rapid changes, with the interaction of the two processes explaining changes in forested area. Results showed minor declines in the abundance of *Picea*, *Larix*, and *Betula* genera, and minor increases in *Pinus*, across the simulation period. Species richness declined for all scenarios, declining the most under more severe disturbances (Figure

5a). The mean number of age classes present at one-hectare sites followed similar patterns but recovered over time for succession-only scenarios (Figure 5b). The central tendency (i.e., median) of the spatial distribution of forests mildly increased in latitude and elevation under the most severe disturbances. While the mean forest latitude increased for all scenarios modeled, mean forest elevation was generally flat or declined (Figures 5c and 5d).

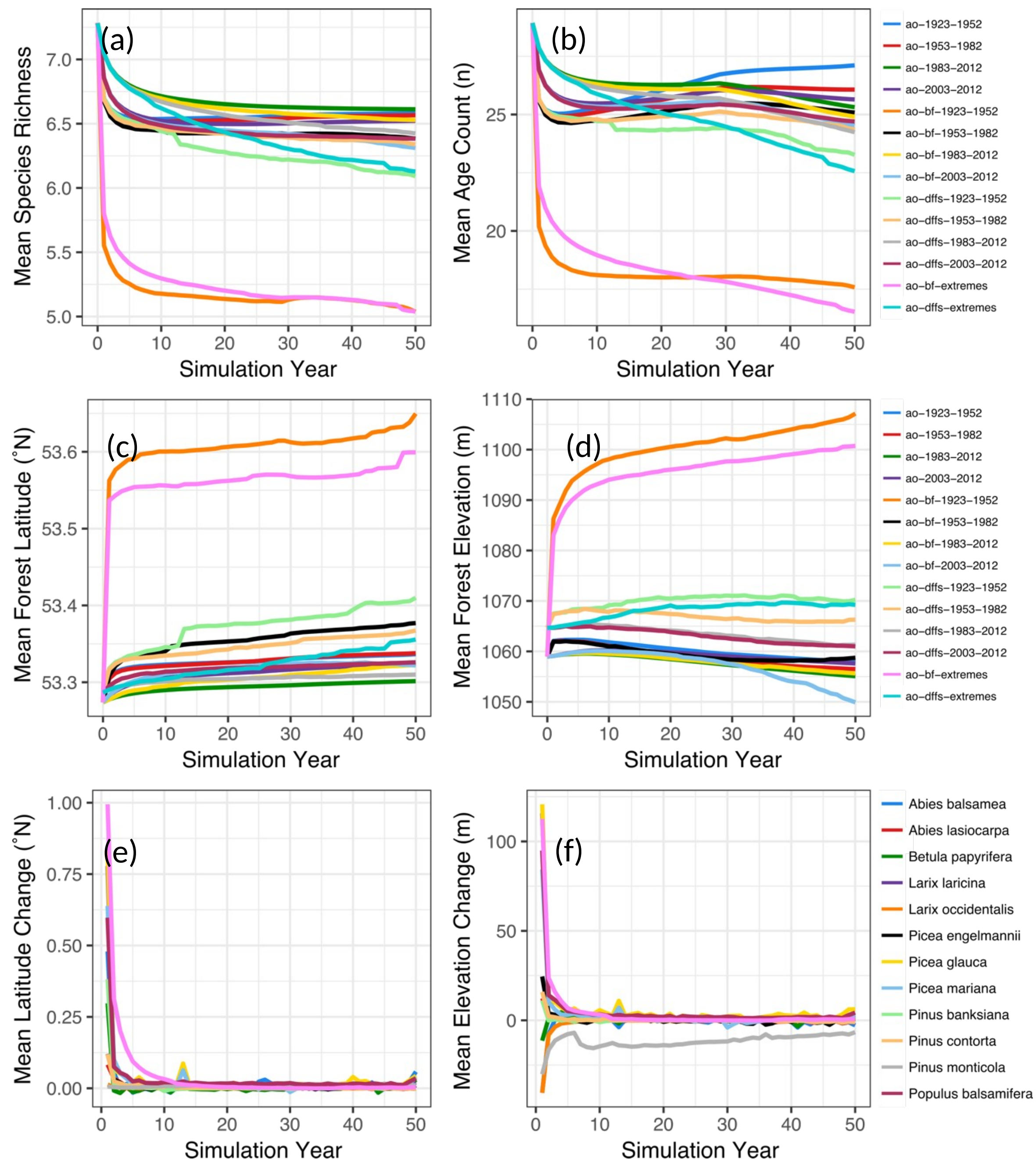

Figure 5. Individual and ensemble (i.e., simulation mean) model results by scenario and species: (a) species richness by scenario; (b) age class count by scenario; (c) mean forest latitude by scenario in WGS84 decimal degrees; (d) mean forest elevation by scenario; (e) incremental mean forest latitude change by species in WGS84 decimal degrees; (f) incremental mean forest elevation change by species; refer to Table S1 for scenario codes

A downhill mean forest distribution shift was shown for the Global Change and Most Recent Decade periods (Figure 5d). This is explained by an increase in high-elevation burning and reduction in regeneration suitability here, due to modeled water holding capacity limitations of rocky soils for the Montane region. A previous analysis of the region showed that available water storage capacity was the most important model predictor of regeneration here (Erickson et al. 2015). In the Pre-Suppression and Extreme scenarios, the spatial distribution of forests shifted uphill on average due to high fire mortality rates at low elevations that surpassed the rate of regeneration. The difference in mean forest elevation between the two scenarios indicates that warming climatic conditions slowed rather than accelerated an uphill mean distribution shift (Figure 5d).

Latitudinal and elevational changes were produced by the spatiotemporal distribution of fire mortality more than climate over the 50-year simulation period. This is evidenced by large incremental changes in species elevation and latitude in the initial simulation years (Figures 5e and 5f), when disturbances were greatest in magnitude. While this spin-up period is often omitted from simulation studies, it is shown here to make model behavior transparent. The weaker effect of warming is also evident in a comparison of Extremes scenarios with Pre-suppression Era fire scenarios, which differed only in climate. Species responses varied in mean latitudinal and elevational distribution shifts resulting from fire. Rather than attributable to life history strategy or functional type, differences in species response appear primarily attributable to the initial location of species. This is evidenced by the observation that the greatest mean species distribution shifts were shown by species endemic to the boreal region, in the northeastern portion of the study area, where the rate of burning was greatest. These changes were particularly evident for the large fires of the base fire scenarios (Figures 5e and 5f).

The velocity of warming outpaced tree migration four-fold

In the full ensemble results (the mean of all scenarios), the mean latitude of forests shifted mildly poleward while the mean elevation was static (mean latitude = +111 m yr^{-1}; mean elevation = -0.02 m yr^{-1}). All periods showed agreement in a mean latitudinal increase in forests, which may partially be explained by recruitment during the model spin-up period. Forest composition remained stable under the two most recent scenarios (Global Change and Most Recent Decade), but less stable during previous scenarios (Pre-Suppression and Early Suppression) due to greater disturbances. Extreme scenarios combining the most area burned with the warmest climatic conditions showed the most rapid changes in forest demographics (Figure 5b) and composition (Supplementary material, Figure S3).

Ensemble model results showed agreement in forested area decline (Supplementary material, Figure S3). An analysis of simulated annual mean incremental changes in area burned, fire frequency, and, forest latitude and elevation (Supplementary material, Figure S4) using Spearman's rank correlation coefficient (ρ) to probe for monotonicity showed that latitudinal and elevational changes were strongly correlated ($\rho = 0.71$), positively correlated with area burned ($\rho = 0.49$; $\rho = 0.34$), and negatively correlated with fire frequency ($\rho = -0.34$; $\rho = -0.50$). Total forested area was negatively correlated with fire frequency more than area burned ($\rho = -0.54$; $\rho = -0.11$) (Supplementary material, Figure S3c).

The periodicity (i.e., autocorrelation) of elevational changes was strongly correlated with changes to fire frequency ($\rho = 0.90$). The periodicity of changes in total forested area was negatively correlated with changes to area burned, fire frequency, and, latitude and elevation ($\rho = -0.32$; $\rho = -0.31$; $\rho = -0.06$; $\rho = -0.24$). The periodicity of changes in mean forest latitude and elevation were positively correlated with changes in area burned and fire frequency, with forest elevation and fire frequency showing the highest correlation (Supplementary material, Figure S3d).

During the model spin-up decade, where age class distributions were initially homogeneous, distributional shifts occurred at their most rapid rate. This result was produced by a combination of high severity boreal fires given an even availability of fuels and frequent initial recruitment events. Given an even initial age class distribution, the sexual maturity of trees had equally even coverage, facilitating seed dispersal. These spin-up patterns are critical to note for their role in influencing the interpretation of simulation results. Following the 10-year model spin-up period, all scenarios with fire showed a mild decline in forested area (Figure 4).

Conclusions

A combination of reduced regeneration potential and more severe fires produced a significant reduction to the total forested area in simulations. This suggests that declining modeled regeneration potential together with reduced burning in the Global Change Era may potentially diminish the ability of tree species to track the velocity of warming. The simulated mean northward shift in forest distribution was 319 m yr^{-1} slower than the velocity of climate change (Loarie et al. 2009; Hamann et al. 2015), with agreement shown across simulations. Even under the greatest burning and thus migration rates, northward forest migration lagged 291 m yr^{-1} behind warming. As exhibited by the Extremes scenarios, migration rates were highest in periods where disturbance rates were the most severe, despite cooler temperatures. This is indicative of reduced competitive limitations to migration.

Changes in the distribution of tree species and forests were primarily attributable to fire. Forests tended to shift toward higher latitudes and lower elevations across simulation scenarios, while higher fire mortality reduced species and age-class diversity. The mean of the spatial distribution of forests increased in elevation and latitude when disturbance severity was highest, facilitating more rapid migrations with the removal of stands. Although shifts in mean spatial distribution were mild, they are notable given the simulation period of fifty years, short relative to the duration of successional processes. Despite being confined within a fixed study area at a regional scale, changes in the mean spatial distribution of forests may be indicative of broader migrational patterns. Changes in the mean spatial distribution of forests are potentially more robust than range minima or maxima as indicators of migrational change, given the larger sample sizes involved and reduced sensitivity to episodic events produced by leptokurtic (i.e., heavy-tailed) seed dispersal kernels.

In addition to fire suppression (Cumming 2005), recent changes to forest demographics may partially explain the empirically observed increase in fire rotation period in Alberta (Zhang et al. 2015), due to the bottom-up nature of fire mortality (i.e., younger cohorts are more susceptible to mortality for a given fire intensity, limiting fire crowning through ladder fuels in the absence of young trees). Fire suppression, forest aging, reduced recruitment rates, and related fire energetic constraints may together explain the modest increase in area burned under warming (Kelly et al. 2013; Héon et al. 2014; Zhang et al. 2015). This dynamic was reproduced in simulations with the elimination of young trees during the model spin-up period, yielding older and less diverse stands with a reduced rate of burning. Simulation results also suggest that, while secondary to fire, declining regeneration potential may play a role in the decline in forested area observed for the Global Change Era in the adjacent montane Western United States (Cohen et al. 2016).

Some studies have indicated increased forest carbon sequestration under global change conditions (Chen et al. 2006; Fang et al. 2014), while a recent tree-ring analysis indicates no effect of warming on biomass increment in the Canadian boreal (Girardin et al. 2016). These projections fail to account for expected changes to fire regimes and tree regeneration under warming. Empirical evidence shows diminished recruitment rates for the region (Zhang et al. 2015), in agreement with TACA model results, while burning is projected to increase under warming in the short-term (Flannigan et al. 2001; Groot et al. 2003), before being limited by energetic constraints (Héon et al. 2014). The presented simulation results indicate that the interaction of higher burn rates and diminishing regeneration potential may offset any potential gains to carbon storage over centennial time-scales by reducing the forested area. This dynamic may also offset increases to forest biomass attributable to stand aging (Huang et al. 2013; Uyeda et al. 2017).

Diminished resilience, or capacity of forests in their current state to respond elastically to perturbation, is evidenced by changes to regeneration, which regulates forest change at a basal physiological level. Although variability in interspecific regeneration potential was evident for the region, the dominant regeneration signal across the study period was a long-term decrease in forested area, in agreement with recent ground plot- and remote sensing-based findings on recruitment and forest cover across the greater region (Bond-Lamberty et al. 2014; Zhang et al. 2015; Cohen et al. 2016). While Zhang *et al.* (2015) attributed reduced growth and recruitment rates in western Canada primarily to competition and secondly to climate, their analysis focused on undisturbed sites, making growth and recruitment rates primarily a function of stand development.

Meanwhile, fire is the dominant driver of mortality in boreal forests (Rowe 1961; Rowe and Scotter 1973; Bond-Lamberty et al. 2007), providing sites for recruitment (Clark 1991; Lavoie and Sirois 1998; Johnstone et al. 2010; Bond-Lamberty et al. 2014), while competition and climate cannot be disentangled. Competitive or mutualistic interactions are a function of climate space, evident in phenotype plasticity (i.e., gene expression) and evolutionary legacies (Aitken et al. 2008). The TACA model results presented herein suggest an alternative interpretation of the results of Zhang *et al.* (2015), as our modeling results indicate that diminished recruitment rates in the western Canadian boreal are due to a climatically-induced decline in regeneration potential.

Combined with available empirical evidence for Canada (Leithead et al. 2012; Fisichelli et al. 2014; Zhang et al. 2015; Cohen et al. 2016), our results suggest that a mild decline in forested area observed for some parts of intermountain western North America in recent decades may be attributable to a combination of increased fire regime severity (i.e., mortality) and diminished regeneration potential. Future studies should explore the interplay of disturbance, dispersal, and regeneration rates in changes to forested area observed for northwest North America. Empirical studies should focus on biome interfaces experiencing the highest rate of forest change. Simulation studies should expand beyond current species ranges to incorporate shifts at the edge of range limits. Improved spaceborne monitoring, data assimilation, and landscape genetic analyses will be important to understanding these dynamics, granting ecological forecasting greater predictive power. By conducting experiments *in silico*, the resilience of forests can be tested under different future scenarios, enabling managers to adjust policies to achieve desired targets. These applications may be considered first steps toward simulation-based management optimization.

Acknowledgements

We sincerely thank our collaborators who made this work possible. Andreas Hamann and Laura Gray of University of Alberta provided tree species distribution data for western Canada. Cordy Tymstra, Ralph Wright, and Bob Mazurik at Government of Alberta, and, Brad Hawkes and Marc-André Parisien at Natural Resources Canada, provided supporting data and guidance on wildfire modeling in Canada. Matthew Duveneck at Harvard University provided guidance on LANDIS-II model implementation, while Brian Miranda and Brian Sturtevant of the USDA Forest Service provided support for the Dynamic Fuels and Fire System. A.E. was generously funded by the Grizzly Bear Program of the Foothills Research Institute located in Hinton, Alberta, Canada. Additional information is available at http://foothillsresearchinstitute.ca. Funding was also provided by an NSERC grant. A.E. led the writing of the paper, acquired data, developed TACA-EM and LANDIS-II parameterization methods for western Canada, conducted the simulations, and analyzed the results. C.N. designed and developed the TACA-EM model and provided all tree species parameters. G.S. contributed to the study design and provided support to conduct the work.

References

Agriculture and Agri-Food Canada (2012) ISO 19131 Land cover for agricultural regions of Canada, circa 2000 – data product specification. Agriculture and Agri-Food Canada, Ottowa, ON, Canada

Aitken SN, Yeaman S, Holliday J a., et al (2008) Adaptation, migration or extirpation: climate change outcomes for tree populations. Evol Appl 1:95–111. doi: 10.1111/j.1752-4571.2007.00013.x

Allen CD, Macalady AK, Chenchouni H, et al (2010) A global overview of drought and heat-induced tree mortality reveals emerging climate change risks for forests. For Ecol Manage 259:660–684. doi: 10.1016/j.foreco.2009.09.001

Andrews PL, Chase CH (1989) BEHAVE: Fire Behavior Prediction and Fuel Modeling System - BURN Subsystem, Part 1. US Department of Agriculture, Forest Service, Washington D.C.

Barton L V. (1930) Hastening the germination of some coniferous seeds. Am J Bot 17:88–115. doi: 10.2307/2446382

Bertrand R, Lenoir J, Piedallu C, et al (2011) Changes in plant community composition lag behind climate warming in lowland forests. Nature 479:517–20. doi: 10.1038/nature10548

Bevington J (1986) Geographic differences in the seed germination of paper birch (Betula papyrifera). Am J Bot 73:564–573. doi: 10.2307/2444262

Bevington JM, Hoyle MC (1981) Phytochrome action during prechilling induced germination of Betula papyrifera Marsh. Plant Physiol 67:705–710. doi: 10.1104/pp.67.4.705

Bond-Lamberty B, Peckham SD, Ahl DE, Gower ST (2007) Fire as the dominant driver of central Canadian boreal forest carbon balance. Nature 450:89–92. doi: 10.1038/nature06272

Bond-Lamberty B, Rocha A V, Calvin K, et al (2014) Disturbance legacies and climate jointly drive tree growth and mortality in an intensively studied boreal forest. Glob Chang Biol 20:216–227. doi: 10.1111/gcb.12404

Boychuk D, Perera AH (1997) Modeling temporal variability of boreal landscape age-classes under different fire disturbance regimes and spatial scales. Can J For Res 27:1083–1094. doi: 10.1139/x97-063

Burns RM, Honkala BH (1990) Silvics of North America. United States Forest Service, Washington

Canadian Forest Service (2015) Canadian Wildland Fire Information System (CWFIS) Datamart. http://cwfis.cfs.nrcan.gc.ca/datamart. Accessed 1 Jan 2015

Carlson CE (1994) Germination and early growth of western larch (Larix occidentalis), alpine larch (Larix lyallii), and their reciprocal hybrids. Can J For Res 24:911–916. doi: 10.1139/x94-120

Chamberlain S, Erickson A, Potter N, et al (2016) rnoaa: “NOAA” Weather Data from R. R package version 0.5.2.

Chen JM, Chen B, Higuchi K, et al (2006) Boreal ecosystems sequestered more carbon in warmer years. Geophys Res Lett 33:. doi: 10.1029/2006GL025919

Chuine I (2010) Why does phenology drive species distribution? Philos Trans R Soc B Biol Sci 365:3149–3160

Chuine I, Beaubien EG (2001) Phenology is a major determinant of tree species range. Ecol Lett 4:500–510. doi: 10.1046/j.1461-0248.2001.00261.x

Clark JS (1991) Disturbance and tree life history on the shifting mosaic landscape. Ecology 72:1102–1118. doi: 10.2307/1940609

Clark JS, Fastie C, Hurtt G, et al (1998) Reid’s paradox of rapid plant migration. Bioscience 48:13–24. doi: 10.2307/1313224

Cohen WB, Yang Z, Stehman S V, et al (2016) Forest disturbance across the conterminous United States from 1985–2012: The emerging dominance of forest decline. For Ecol Manage 360:242–252. doi: http://dx.doi.org/10.1016/j.foreco.2015.10.042

Cumming SG (2005) Effective fire suppression in boreal forests. Can J For Res 35:772–786. doi: 10.1139/x04-174

Davis MB, Shaw RG (2001) Range shifts and adaptive responses to Quaternary climate change. Science (80-) 292:673–679. doi: 10.1126/science.292.5517.673

DeByle N V., Winokur RP (1985) Aspen: Ecology and management in the western United States. US Department of Agriculture, Forest Service, Fort Collins, CO, USA

Dempster AP, Laird NM, Rubin DB (1977) Maximum Likelihood from Incomplete Data via the EM Algorithm. J R Stat Soc Ser B 39:1–38

Derr BD, Matelski RP, Peterson GW (1969) Soil factors influencing percolation test performance. Soil Sci Soc Am Proc 33:942–946

Dilley a. C, Millie S, O'Brien DM, et al (2004) The relation between Normalized Difference Vegetation Index and vegetation moisture content at three grassland locations in Victoria, Australia. Int J Remote Sens 25:3913–3930. doi: 10.1080/01431160410001698889

Dobbs RC (1976) White spruce seed dispersal in central British Columbia. For Chron 52:30–33

Dreyfus S (1962) The numerical solution of variational problems. J Math Anal Appl 5:30–45. doi: http://dx.doi.org/10.1016/0022-247X(62)90004-5

Edwards DGW (1982) Improving seed germination in Abies. In: International Plant Propagators' Society Combined Proceedings for 1981. Canadian Forest Service, Richmond, B.C., pp 69-78 (Volume 31)

Erickson AM, Nitschke CR, Coops NC, et al (2015) Past-century decline in forest regeneration potential across a latitudinal and elevational gradient in Canada. Ecol Modell 313:94–102. doi: http://dx.doi.org/10.1016/j.ecolmodel.2015.06.027

Fang J, Kato T, Guo Z, et al (2014) Evidence for environmentally enhanced forest growth. Proc Natl Acad Sci 111:9527–9532. doi: 10.1073/pnas.1402333111

Farmer RE, Charrette P, Searle IE, Tarjan DP (1984) Interaction of light, temperature, and chilling in the germination of black spruce. Can J For Res 14:131–133. doi: 10.1139/x84-025

Farrar JL (1995) Trees in Canada, 3rd edn. Fitzhenry & Whiteside Ltd., Ottawa, ON, Canada

Feurtado JA, Ambrose S, Cutler A, et al (2004) Dormancy termination of western white pine (Pinus monticola Dougl. Ex D. Don) seeds is associated with changes in abscisic acid metabolism. Planta 218:630–639. doi: 10.1007/s00425-003-1139-8

Finney MA (2004) FARSITE: Fire Area Simulator - model development and evaluation. Ogden, UT, USA

Finney MA (2002) Fire growth using minimum travel time methods. Can J For Res 32:1420–1424

Fisichelli NA, Frelich LE, Reich PB (2014) Temperate tree expansion into adjacent boreal forest patches facilitated by warmer temperatures. Ecography (Cop) 37:152–161. doi: 10.1111/j.1600-0587.2013.00197.x

Flannigan M, Campbell I, Wotton M, et al (2001) Future fire in Canada's boreal forest: paleoecology results and general circulation model - regional climate model simulations. Can J For Res 31:854–864. doi: 10.1139/x01-010

Flannigan MD, Wotton BM (1994) Fire regime and the abundance of jack pine. In: Proceedings of the 2nd International Conference on Forest Fire Research. University of Coimbra, Coimbra, Portugal, pp 625-639 (Vol. II, C.09)

Forestry Canada Fire Danger Group (1992) Development and structure of the Canadian Forest Fire Behavior Prediction System. Ottowa, ON, Canada

Girardin MP, Bouriaud O, Hogg EH, et al (2016) No growth stimulation of Canada's boreal forest under half-century of combined warming and CO2 fertilization. Proc Natl Acad Sci 113:E8406–E8414. doi: 10.1073/pnas.1610156113

Government of Alberta (2009) Gene Conservation Plan for Native Trees of Alberta

Gray LK, Hamann A (2012) Tracking suitable habitat for tree populations under climate change in western North America. Clim Change 117:289–303. doi: 10.1007/s10584-012-0548-8

Greenwood MS, Livingston WH, Day ME, et al (2002) Contrasting modes of survival by jack and pitch pine at a common range limit. Can J For Res 32:1662–1674. doi: 10.1139/x02-088

Greenwood MS, O'Brien CL, Schatz JD, et al (2008) Is early life cycle success a determinant of the abundance of red spruce and balsam fir? Can J For Res 38:2295–2305. doi: 10.1139/X08-072

Grenier M, Sirois L (2009) Reproductive development and seed ripening in Betula papyrifera along an altitudinal thermal gradient in eastern Appalachia (Canada). Botany 87:492–500. doi: 10.1139/B09-018

Groot WJ, Bothwell PM, Carlsson DH, Logan K a. (2003) Simulating the effects of future fire regimes on western Canadian boreal forests. J Veg Sci 14:355–364. doi: 10.1111/j.1654-1103.2003.tb02161.x

Hamann A, Roberts DR, Barber QE, et al (2015) Velocity of climate change algorithms for guiding conservation and management. Glob Chang Biol 21:997–1004. doi: 10.1111/gcb.12736

Hargreaves GH, Samani ZA (1985) Reference Crop Evapotranspiration from Temperature. Appl Eng Agric 1:

Harrell FEJ, Dupont C (2015) Hmisc: Harrell miscellaneous

He HS, Mladenoff DJ (1999) Spatially explicit and stochastic simulation of forest-landscape fire disturbance and succession. Ecology 80:81–99. doi: 10.2307/176981

Héon J, Arseneault D, Parisien M-A (2014) Resistance of the boreal forest to high burn rates. Proc Natl Acad Sci 111:13888–13893. doi: 10.1073/pnas.1409316111

Hirsch KG (1993) A brief overview of the Canadian Forest Fire Behavior Prediction (FBP) System. Int Assoc Wildl Fire HotSheet 2:3

Hogg EH (1994) Climate and the Southern Limit of the Western Canadian Boreal Forest. Can J For Res 24:

Hogg EH (Ted), Brandt JP, Michaelian M (2008) Impacts of a regional drought on the productivity, dieback, and biomass of western Canadian aspen forests. Can J For Res 38:1373–1384. doi: 10.1139/X08-001

Holling CS (1978) Adaptive Environmental Assessment and Management. John Wiley & Sons, Chichester, UK

Honaker J, King G, Blackwell M (2011) Amelia II: A program for missing data. J Stat Softw 45:47

Huang S, Liu H, Dahal D, et al (2013) Modeling spatially explicit fire impact on gross primary production in interior Alaska using satellite images coupled with eddy covariance. Remote Sens Environ 135:178–188. doi: http://dx.doi.org/10.1016/j.rse.2013.04.003

Huang S, Titus SJ, Wiens DP (1992) Comparison of nonlinear height–diameter functions for major Alberta tree species. Can J For Res 22:1297–1304. doi: 10.1139/x92-172

Jelinski DE, Cheliak WM, Society B, et al (1992) Genetic diversity and spatial subdivision of Populus tremuloides (Salicaceae) in a heterogeneous landscape. Am J Bot 79:728–736

Johnstone JF, Hollingsworth TN, Chapin FS, Mack MC (2010) Changes in fire regime break the legacy lock on successional trajectories in Alaskan boreal forest. Glob Chang Biol 16:1281–1295. doi: 10.1111/j.1365-2486.2009.02051.x

Junger W, de Leon AP (2012) mtsdi: Multivariate time series data imputation

Keeley JE, Pausas JG, Rundel PW, et al (2014) Fire as an evolutionary pressure shaping plant traits. Trends Plant Sci 16:406–411. doi: 10.1016/j.tplants.2011.04.002

Kelly R, Chipman ML, Higuera PE, et al (2013) Recent burning of boreal forests exceeds fire regime limits of the past 10,000 years. Proc Natl Acad Sci 110:13055–13060. doi: 10.1073/pnas.1305069110

Kimmins H, Blanco JA, Seely B, et al (2010) Forecasting Forest Futures: A Hybrid Modelling Approach to the Assessment of Sustainability of Forest Ecosystems and Their Values. Taylor & Francis Group

Klinka K, Worrall J, Skoda L, Varga P (2000) The Distribution and Synopsis of Ecological and Silvical Characteristics of Tree Species of British Columbia’s Forests. Canadian Cartographics Ltd., Coquitlam, BC, Canada

Lavoie L, Sirois L (1998) Vegetation changes caused by recent fires in the northern boreal forest of eastern Canada. J Veg Sci 9:483–492. doi: 10.2307/3237263

Lazarus ED, McGill BJ (2014) Pushing the pace of tree species migration. PLoS One 9:e105380

Leadem CL (1989) Stratification and quality assessment of Abies lasiocarpa seeds. Canada-BC Economic & Regional Development Agreement, Victoria, BC, Canada

Leadem CL (1985) Seed dormancy in three Pinus species of the inland mountain west. In: Shearer RC (ed) Conifer Tree Seed in the Inland Mountain West Symposium. US

Department of Agriculture, Forest Service, Ogden, UT, USA, pp 117–123

LeCun Y, Bengio Y, Hinton G (2015) Deep learning. Nature 521:436–444

Leithead M, Silva LR, Anand M (2012) Recruitment patterns and northward tree migration through gap dynamics in an old-growth white pine forest in northern Ontario. Plant Ecol 213:1699–1714. doi: 10.1007/s11258-012-0116-3

Li XJ, Burton PJ, Leadem CL (1994) Interactive effects of light and stratification on the germination of some British Columbia conifers. Can J Bot 72:1635–1646

Linnainmaa S (1970) The representation of the cumulative rounding error of an algorithm as a Taylor expansion of the local rounding errors. University of Helsinki

Loarie SR, Duffy PB, Hamilton H, et al (2009) The velocity of climate change. Nature 462:1052–5. doi: 10.1038/nature08649

Lotan JE, Perry DA (1983) Ecology and Regeneration of Lodgepole Pine

Martínez-Vilalta J, Lloret F, Breshears DD (2012) Drought-induced forest decline: Causes, scope and implications. Biol Lett 8:689–691. doi: 10.1098/rsbl.2011.1059

Mascaro J, Hughes RF, Schnitzer SA (2011) Novel forests maintain ecosystem processes after the decline of native tree species. Ecol Monogr 82:221–228. doi: 10.1890/11-1014.1

Matzke MA, Mosher RA (2014) RNA-directed DNA methylation: An epigenetic pathway of increasing complexity. Nat Rev Genet 15:394–408

McCune B, Allen TFH (1985) Forest dynamics in the Bitterroot Callyons, Montana. Can J Bot 63:377–383

Menne MJ, Durre I, Vose RS, et al (2012) An overview of the Global Historical Climatology Network-Daily database. J Atmos Ocean Technol 29:897–910. doi: 10.1175/JTECH-D-11-00103.1

Meunier C, Sirois L, Bégin Y (2007) Climate and Picea mariana seed maturation relationships: A multi-scale perspective. Can J For Res 77:361–376. doi: 10.1890/06-1543.1

Michaelian M, Hogg EH, Hall RJ, Arsenault E (2011) Massive mortality of aspen following severe drought along the southern edge of the Canadian boreal forest. Glob Chang Biol 17:2084–2094. doi: 10.1111/j.1365-2486.2010.02357.x

Mladenoff DJ, He HS (1999) Design, behavior and application of LANDIS, an object-oriented model of forest landscape disturbance and succession. In: Spatial Modeling of Forest Landscape Change: Approaches and Applications. Cambridge University Press, Cambridge, UK, pp 125–162

Mladenoff DJ, Host GE, Boeder J, Crow TR (1993) LANDIS: a spatial model of forest landscape disturbance, succession, and management. In: Second International Conference on Integrating Modelling and GIS

Moss EH (2012) The Vegetation of Alberta. Bot Rev 21:493–567. doi: 10.1007/BF02872442

Natural Regions Committee (2006) Natural Regions and Subregions of Alberta. Government of Alberta, Edmonton, AB, Canada

Nitschke CR, Amoroso M, Coates KD, Astrup R (2012) The influence of climate change, site type, and disturbance on stand dynamics in northwest British Columbia, Canada. Ecosphere 3:11. doi: 10.1890/ES11-00282.1

Nitschke CR, Innes JL (2008) A tree and climate assessment tool for modelling ecosystem response to climate change. Ecol Modell 210:263–277. doi: 10.1016/j.ecolmodel.2007.07.026

Nitschke CR, Innes JL, Biology GC (2008) Climatic change and fire potential in south-central British Columbia, Canada. Glob Chang Biol 14:841–855. doi: 10.1111/j.1365-2486.2007.01517.x

Organisation for Economic Co-operation and Development (2006) Consensus Document on the Biology of Western White Pine (Pinus monticola Dougl. Ex D. Don). Paris, France

Owens JN, Bruns D (2000) Western white pine (Pinus monticola Dougl.) reproduction: I. Gametophyte development. Sex Plant Reprod 13:61–74. doi: 10.1007/s004970000042

Parminter J (1984) Fire-ecological relationships for the biogeoclimatic zones of the northern portion of the Mackenzie Timber Supply Area: summary report. British Columbia Ministry of Forests, Victoria, BC, Canada

Peterson EB, Peterson NM, Simard SW, Wang JR (1997) Paper Birch Managers Handbook for British Columbia. Natural Resources Canada, Victoria, BC, Canada

Pickett STA, Thompson JN (1978) Patch dynamics and the design of nature reserves. Biol Conserv 13:27–37. doi: http://dx.doi.org/10.1016/0006-3207(78)90016-2

Pitel JA, Cheliak WM (1986) Enzyme activities during imbibition and germination of seeds of tamarack (Larix laricina). Physiol Plant 67:562–569. doi: 10.1111/j.1399-3054.1986.tb05056.x

Pounden E, Greene DF, Michaletz ST (2014) Non-serotinous woody plants behave as aerial seed bank species when a late-summer wildfire coincides with a mast year. Ecol Evol 4:3830–3840. doi: 10.1002/ece3.1247

Prentice IC (1986) Vegetation responses to past climatic variation. Vegetatio 67:131–141. doi: 10.1007/BF00037363

R Core Team (2015) R: A Language and Environment for Statistical Computing

Renault S, Zwiazek JJ, Fung M, Tuttle S (2000) Germination, growth and gas exchange of selected boreal forest seedlings in soil containing oil sands tailings. Environ Pollut 107:357–365. doi: http://dx.doi.org/10.1016/S0269-7491(99)00167-0

Rogers BM, Soja AJ, Goulden ML, Randerson JT (2015) Influence of tree species on continental differences in boreal fires and climate feedbacks. Nat Geosci 8:228–234

Rowe JS (1961) Critique of some vegetational concepts as applied to forests of northwestern Alberta. Can J Bot 39:

Rowe JS, Scotter GW (1973) Fire in the boreal forest. Quat Res 3:444–464. doi: http://dx.doi.org/10.1016/0033-5894(73)90008-2

Scheller RM, Domingo JB, Sturtevant BR, et al (2007) Design, development, and application of LANDIS-II, a spatial landscape simulation model with flexible temporal and spatial resolution. Ecol Modell 201:409–419. doi: 10.1016/j.ecolmodel.2006.10.009

Scheller RM, Mladenoff DJ (2004) A forest growth and biomass module for a landscape simulation model, LANDIS: design, validation, and application. Ecol Modell 180:211–229. doi: http://dx.doi.org/10.1016/j.ecolmodel.2004.01.022

Schwilk DW, Ackerly DD (2001) Flammability and serotiny as strategies: correlated evolution in pines. Oikos 94:326–336. doi: 10.1034/j.1600-0706.2001.940213.x

Simons-Legaard E, Legaard K, Weiskittel A (2015) Predicting aboveground biomass with LANDIS-II: a global and temporal analysis of parameter sensitivity. Ecol Modell 313:325–332. doi: http://dx.doi.org/10.1016/j.ecolmodel.2015.06.033

Sirois L (2000) Spatiotemporal variation in black spruce cone and seed crops along a boreal forest - tree line transect. Can J For Res 30:900–909. doi: 10.1139/x00-015

Soil Classification Working Group (1998) The Canadian System of Soil Classification, 3rd edn. Canadian Science Publishing, Ottowa, ON, Canada

Soil Landscapes of Canada Working Group (2010) Soil landscapes of Canada version 3.2. In: Can. Soil Inf. Syst. http://sis.agr.gc.ca/cansis/nsdb/slc/v3.2/index.html. Accessed 1 Jan 2015

Sorenson FC (1990) Stratification requirements for germination of western larch (Larix occidentalis Nutt.) seed. US Department of Agriculture, Forest Service, Portland, OR, USA

Spies TA, Franklin JF (1989) Gap Characteristics and Vegetation Response in Coniferous Forests of the Pacific Northwest. Ecology 70:543-545 CR-Copyright © 1989 Ecological Soc. doi: 10.2307/1940198

Stanek W (1961) Natural layering of black spruce in Northern Ontario. For Chronical 37:245–258. doi: 10.5558/tfc37245-3

Sturtevant BR, Scheller RM, Miranda BR, et al (2009) Simulating dynamic and mixed-severity fire regimes: a process-based fire extension for LANDIS-II. Ecol Modell 220:3380–3393. doi: http://dx.doi.org/10.1016/j.ecolmodel.2009.07.030

Syphard AD, Yang J, Franklin J, et al (2007) Calibrating a forest landscape model to simulate frequent fire in Mediterranean-type shrublands. Environ Model Softw 22:1641–1653. doi: http://dx.doi.org/10.1016/j.envsoft.2007.01.004

Thompson RS, Anderson KH, Bartlein PJ (1999) Atlas of relations between climatic parameters and distributions of important trees and shrubs in North America. US Geological Survey, Washington, DC, USA

Tymstra C, Bryce RW, Wotton BM, et al (2010) Development and structure of Prometheus: the Canadian wildland fire growth simulation model. Edmonton, AB, Canada

United States Forest Service (2013) Species: Populus tremuloides. In: Fire Eff. Inf. Syst. https://www.fs.fed.us/database/feis/plants/tree/poptre/all.html. Accessed 1 Jan 2015

Uyeda KA, Stow DA, Roberts DA, Riggan PJ (2017) Combining ground-based measurements and MODIS-based spectral vegetation indices to track biomass accumulation in post-fire chaparral. Int J Remote Sens 38:728–741. doi: 10.1080/01431161.2016.1271477

van Mantgem PJ, Stephenson NL, Byrne JC, et al (2009) Widespread increase of tree mortality rates in the western United States. Science 323:521–4. doi: 10.1126/science.1165000

Van Wagner CE (1989) Prediction of crown fire in conifer stands. In: MacIver DC, Auld H, Whitewood R (eds) Proceedings of the 10th Conference on Fire and Forest Meteorology. Forestry Canada, Ottowa, ON, Canada, pp 207–212

Van Wagner CE (1987) Development and structure of the Canadian Forest Fire Weather Index System. Natural Resources Canada, Ottowa, Ontario

Vilà-Cabrera A, Martínez-Vilalta J, Galiano L, Retana J (2013) Patterns of forest decline and tegeneration across Scots pine populations. Ecosystems 16:323–335. doi: 10.1007/s10021-012-9615-2

von Neumann J (1966) Theory of Self-Reproducing Automata. University of Illinois Press, Urbana and London

Wagner CE Van (1977) Conditions for the start and spread of crown fire. Can J For Res 7:23–34. doi: 10.1139/x77-004

Wang T, Hamann A, Spittlehouse DL, Aitken SN (2006) Development of Scale-Free Climate Data for Western Canada for Use in Resource Management. 397:383–397. doi: 10.1002/joc.1247

Wang X, Cantin A, Parisien M-A, et al (2014) fwi.fbp: Fire Weather Index System and Fire Behaviour Prediction System calculations

Ward BC, Scheller RM, Mladenoff DJ (2004) Technical Report: LANDIS-II Double Exponential Seed Dispersal Algorithm. Dept. Forest Ecology and Management, University of Wisconsin-Madison, Madison, WI, USA

Waring RH, Running SW (1998) Forest Ecosystems: Analysis at Multiple Scales. Academic Press, Amsterdam; Boston

White JM, Mathewes RW (1986) Postglacial vegetation and climatic change in the upper Peace River district, Alberta. Can J Bot 64:2305–2318. doi: 10.1139/b86-302

Widrow B, Hoff M (1960) Adaptive switching circuits. Stanford University, Stanford Electronics Laboratory, Stanford, California

Wolken JM, Landhäusser SM, Lieffers VJ, Dyck MF (2010) Differences in initial root development and soil conditions affect establishment of trembling aspen and balsam poplar seedlings. Botany 88:275–285. doi: 10.1139/B10-016

Woodard PM (1983) Germination success of Pinus contorta Dougl. and Picea Engelmannii Parry on burned seedbeds. For Ecol Manage 5:301–306. doi: http://dx.doi.org/10.1016/0378-1127(83)90034-8

Worrall JJ, Rehfeldt GE, Hamann A, et al (2013) Recent declines of Populus tremuloides in North America linked to climate. For Ecol Manage 299:35–51. doi: 10.1016/j.foreco.2012.12.033

Wulder MA, Cranny M, Hall RJ, et al (2007) Satellite land cover mapping of Canada's forests: the EOSD Land Cover Project. In: North American Land Cover Summit. Natural Resources Canada, Washington DC, USA, pp 21–30

Xu C, Güneralp B, Gertner G, Scheller R (2010) Elasticity and loop analyses: tools for understanding forest landscape response to climatic change in spatial dynamic models. Landsc Ecol 25:855–871. doi: 10.1007/s10980-010-9464-3

Yang J, He HS, Gustafson EJ (2004) A hierarchical fire frequency model to simulate temporal patterns of fire regimes in LANDIS. Ecol Modell 180:119–133. doi: http://dx.doi.org/10.1016/j.ecolmodel.2004.03.017

Zhang J, Huang S, He F (2015) Half-century evidence from western Canada shows forest dynamics are primarily driven by competition followed by climate. Proc Natl Acad Sci 112:4009–4014. doi: 10.1073/pnas.1420844112

Supplementary Material

The TACA-EM model is designed to assess climate change impacts on the regeneration niche, the niche most sensitive to climatic change (Nitschke and Innes 2008). In TACA-EM, regeneration is a function of the biophysical space of each species in relation to soils and daily weather. Each year is simulated at daily resolution to capture phenologically driven regeneration events. Phenology is an important driver of species distributions (Chuine and Beaubien 2001) and plant fitness (Chuine 2010), necessitating its inclusion. Regeneration carries particular importance in global change studies, as it regulates directional change at the lowest level (Fisichelli et al. 2014).

The LANDIS-II model is a hybrid model (i.e., empirical, process-based, and stochastic) of forest dynamics (Kimmins et al. 2010) designed to operate at a stand resolution (~one hectare) and a landscape scale (~10^6 hectares) (Scheller et al. 2007). The LANDIS-II model applies life history strategies within a cellular automaton (von Neumann 1966) using a stochastic number generator and rules-based processes within and across two-dimensional probability matrices or grids. We combined TACA-EM within LANDIS-II to generate species regeneration probabilities under different conditions. Within LANDIS-II, fire is modeled as a blend of stochastic, empirical, mechanistic, and rules-based processes. By coupling TACA-EM with LANDIS-II, we are able to explicitly model forest dynamics under global change.

TACA-EM

Model Overview

The TACA-EM model simulates tree species regeneration as a function of climatic and edaphic conditions relative to species biophysical constraints, as previously described (Nitschke and Innes 2008). TACA-EM relies upon empirically derived biophysical relationships for specific regeneration processes in a process-based approach. The model incorporates species parameters for growing degree days, temperature thresholds, chilling requirements, bud break, drought, and frost. Modeled species navigate biologically relevant thresholds in order to regenerate each year. The overall regeneration probability is the sum of these probabilities divided by the number of scenarios in each simulation, producing an average probability for a given decade. Unlike Bayesian methods, TACA-EM explicitly represents biological processes known to be critical to regeneration. As such, TACA-EM is more likely to maintain model realism under novel conditions where *a priori* information is unavailable.

Model Requirements

In addition to species biophysical parameters, TACA-EM requires daily weather, soils, and solar radiation parameters for each site modeled. The parameters are decadal-scale daily resolution temperature minima and maxima, precipitation, soil moisture regime, soil texture, rooting zone depth, coarse fragment percent, percolation rate, an optional nitrogen modifier for productivity, and latitude. Within TACA-EM, solar radiation and evapotranspiration are calculated using existing formulations (Hargreaves and Samani 1985; Waring and Running 1998). Soil available water storage capacity and annual heat moisture index are modeled using equations incorporating vapor pressure deficit (Wang et al. 2006). Available water storage capacity is the most sensitive model variable; when it falls to zero, soils are assumed to be at the permanent wilting point, below the minimum amount of soil moisture required to prevent permanent turgor loss. TACA-EM produces a drought index as a function of the actual-to-potential evapotranspiration ratio within a soil moisture submodel. The model includes species-specific phenology events, such as bud break, winter hardening, growing season length, and the occurrence of physiological drought and frost at critical times during development.

Model Parameterization

We wrote custom R functions (R Core Team 2015) to download and process NOAA Global Historical Climate Network-Daily (GHCN-Daily) data (Menne et al. 2012), subsequently released within the *rnoaa* package (Chamberlain et al. 2016). Our scripts produce daily resolution temperature and precipitation values for each biogeoclimatic region as the mean of all station values within a region for each day. We utilized the expectation-maximization (EM) algorithm (Dempster et al. 1977) to impute missing values with the R *FastImputation* package, based on Amelia-II (Honaker et al. 2011).

We used the National Soil Database Soil Landscapes of Canada (SLC) v3.2 (Soil Landscapes of Canada Working Group 2010) to generate soil parameters for Natural Subregions of Alberta (Natural Regions Committee 2006) (Supplementary material, Table S1). Soil texture, rooting zone depth, coarse fragment percent, and available water soil capacity were derived from the SLC database for the dominant soil types. We used the Canadian System of Soil

Classification (Soil Classification Working Group 1998) to produce textural classes for these soil types before deriving percolation rates for textural classes from the literature (Derr et al. 1969). Elevational and latitudinal parameters were sourced from a provincial report (Natural Regions Committee 2006) and verified in ArcGIS using 90-meter NASA SRTM data. Our TACA-EM parameterization method is the first to offer climate and soils parameters Canada-wide.

Tree species biophysical attributes were derived from previous studies (Nitschke and Innes 2008; Nitschke et al. 2012) and the literature. Species parameters include physiological base temperature, heat sum for bud break, chilling requirements, minimum temperature, drought tolerance, growing-degree-day minima and maxima, frost tolerance, frost season, wet soils, and heat moisture index responses (Supplementary material, Table S2).

Tree species biophysical parameters were derived from the following literature sources: balsam fir (*Abies balsamea*) (Burns and Honkala 1990; Thompson et al. 1999; Greenwood et al. 2008); subalpine fir (*Abies lasiocarpa*) (Edwards 1982; Leadem 1989; Burns and Honkala 1990; Li et al. 1994; Thompson et al. 1999; Klinka et al. 2000; Nitschke and Innes 2008; Nitschke et al. 2012); white birch (*Betula papyrifera*) (Bevington and Hoyle 1981; Bevington 1986; Burns and Honkala 1990; Thompson et al. 1999; Klinka et al. 2000; Nitschke and Innes 2008; Grenier and Sirois 2009); tamarack (*Larix laricina*) (Pitel and Cheliak 1986; Burns and Honkala 1990; Thompson et al. 1999; Klinka et al. 2000); western larch (*Larix occidentalis*) (Burns and Honkala 1990; Sorenson 1990; Li et al. 1994; Carlson 1994; Thompson et al. 1999; Klinka et al. 2000; Nitschke and Innes 2008); Engelmann spruce (*Picea engelmannii*) (Woodard 1983; Burns and Honkala 1990; Thompson et al. 1999; Klinka et al. 2000; Nitschke and Innes 2008); white spruce (*Picea glauca*) (Burns and Honkala 1990; Li et al. 1994; Thompson et al. 1999; Klinka et al. 2000; Renault et al. 2000; Nitschke and Innes 2008; Nitschke et al. 2012); black spruce

(*Picea mariana*) (Farmer et al. 1984; Burns and Honkala 1990; Thompson et al. 1999; Klinka et al. 2000; Sirois 2000; Meunier et al. 2007; Nitschke and Innes 2008); jack pine (*Pinus banksiana*) (Burns and Honkala 1990; Thompson et al. 1999; Klinka et al. 2000; Renault et al. 2000; Greenwood et al. 2002); lodgepole pine (*Pinus contorta*) (Barton 1930; Woodard 1983; Burns and Honkala 1990; Li et al. 1994; Thompson et al. 1999; Klinka et al. 2000; Nitschke and Innes 2008; Nitschke et al. 2012); western white pine (*Pinus monticola*) (Barton 1930; Leadem 1985; Burns and Honkala 1990; Li et al. 1994; Thompson et al. 1999; Klinka et al. 2000; Feurtado et al. 2004; Nitschke and Innes 2008); balsam poplar (*Populus balsamifera*) (Burns and Honkala 1990; Thompson et al. 1999; Klinka et al. 2000; Nitschke and Innes 2008; Wolken et al. 2010; Nitschke et al. 2012); trembling aspen (*Populus tremuloides*) (Burns and Honkala 1990; Thompson et al. 1999; Klinka et al. 2000; Nitschke and Innes 2008; Wolken et al. 2010; Nitschke et al. 2012).

LANDIS-II

Model Overview

The LANDIS-II model is based on the JABOWA-FORET genre of gap models and LANDSIM (Mladenoff and He 1999). The model incorporates dynamics important at the landscape scale. The LANDIS-II model core is the central hub of a modular system that allows users to specify submodels at a user-defined time-step. In LANDIS-II, each grid cell in the landscape matrix is either active or inactive. Inactive cells are static and active cells are dynamic. Active grid cells can be forested or non-forested. Grasslands are typically the only active non-forested cells, where trees may establish given favorable conditions. Each active forested grid cell is a stand of trees comprised of horizontally homogeneous species-age cohort classes

(Scheller et al. 2007). To better represent variation in regional climate, soils, and fire, we divided the landscape into biogeoclimatic regions. In our simulations, we utilize three submodel configurations: Age-Only Succession, Base Fire, and the Dynamic Fuels and Fire System.

We used the Age-Only Succession submodel to model light, reproduction, ontogeny, senescence, seed dispersal, and interspecific competition. In LANDIS-II, light is modeled as a function of the maximum shade tolerance for sexually mature species present at a site. The presence of shade tolerant species, which fare poorly in open stands (Spies and Franklin 1989), are used as an indicator of poor light conditions. When fires initiate within a cell, younger, more shade tolerant species typically have higher mortality rates, increasing modeled light values.

Reproduction is limited by propagule presence and light availability given regeneration probabilities output from TACA-EM. Fire directly interacts with regeneration through mortality, resprouting, and serotiny. Cohort mortality is a function of species maximum age, with an increasing probability of mortality once species reach 80% of their maximum age. Seed dispersal is represented by a two-part negative exponential probability distribution with a leptokurtic dispersal kernel (Ward et al. 2004), based on observed migration rates (Clark et al. 1998). Interspecific competition occurs through the intersection of species life history attributes, establishment probabilities, and local disturbance patterns.

We apply two conceptually different LANDIS-II extensions for modeling wildfire: Base Fire and the Dynamic Fuels and Fire System. Base Fire is an empirically based stochastic fire-growth model that reproduces parameterized statistical distributions, with variability a result of its stochastic core. In contrast, the Dynamic Fuels and Fire System is a semi-mechanistic stochastic fire-growth model that uses topography, fuel conditions, fire weather, and empirical fire distributions to shape fire patterns. The Dynamic Fuels and Fire System is conceptually analogous to Prometheus in Canada (Tymstra et al. 2010) and FARSITE in the US (Finney 2004), which are based on the Fire Behaviour Prediction (FBP) System (Forestry Canada Fire Danger Group 1992) and BEHAVE (Andrews and Chase 1989), respectively. In both LANDIS-II fire models, fires begin through separate ignition and initiation events (Yang et al. 2004). Mean fire return intervals (Pickett and Thompson 1978) are used to model fire frequency.

In the Base Fire model, the frequency of ignitions follows a Poisson distribution. Fire initiation is based on Bernoulli trials, with ignition probability a function of time-since-last-fire. Fire sizes are drawn from a log-normal distribution (Yang et al. 2004), producing periodic large fires. Fire shape is a product of a stochastic percolation algorithm representing wind vectors. Inactive cells may act as fire breaks, stopping fire spread before reaching its target size. Fire severity is determined by fuel and wind curves representing fuel buildup and decay; a site's position on these curves is determined by time-since-last-fire. Fire is modeled as a bottom-up disturbance, whereby younger cohorts have a higher probability of mortality (He and Mladenoff 1999).

The Dynamic Fuels and Fire System is a process-based fire model that uses a semi-mechanistic representation of fire growth (Sturtevant et al. 2009). Similar to Base Fire, fires are hierarchically split into ignition and initiation events (Yang et al. 2004). Ignition frequency also follows a Poisson distribution, with cells in each fire region selected stochastically. Unlike Base Fire, fire initiation is modeled probabilistically based on site fuel conditions, calculated using cohort information and daily weather data within FBP and Fire Weather Index (FWI) Systems equations (Van Wagner 1987; Forestry Canada Fire Danger Group 1992). Fire sizes are drawn from a log-normal distribution, while users can alternatively specify duration-based sizes. Fire shape is modeled using fuel-specific rate-of-spread equations (Hirsch 1993) and a modified minimal-travel-time cost-path method. The minimum-travel-time method is based on Huygens' Principle of wave propagation, also used in Prometheus and FARSITE. Yet, LANDIS-II implements the most efficient algorithm of the three fire simulators (Finney 2002).

In the Dynamic Fuels and Fire System, the fire spread algorithm contains two core components: wind bias and fuel conditions. Wind bias has an ellipsoidal shape with the length and width based on the magnitude of a wind velocity vector (Finney 2002). Fuel-based spread is a function of fuel class, wind speed, and topography, using FBP System fuel classes. A cost surface is created using the inverse rate-of-spread to calculate a minimum-travel-time path. The cumulative minimum-travel-time and fire size selected determine the shape of each fire, producing improved disturbance pattern realism.

The probability of fire sizes being selected from the log-normal size distribution are classified into five equally spaced bins. These bins correspond to five fire weather bins, based on the logic that larger fires occur during more severe fire weather conditions. The fire weather bins are typically parameterized by classifying FWI values. The seasonal distribution of fire frequency is represented probabilistically, incorporating leaf status. Detailed model information and equations are provided in the literature (Forestry Canada Fire Danger Group 1992; Finney 2002; Sturtevant et al. 2009). Model requirements are provided in the supplementary materials.

Model Requirements

The LANDIS-II model core requires a list containing life history attributes for tree species. These attributes include species longevity, sexual maturity age, shade tolerance, fire tolerance, seed dispersal, vegetative reproduction, and serotiny. The model core also requires a matrix and lookup table specifying tree species-age cohort classes present in each cell. Cohort classes are dynamically updated at each time step. A biogeoclimatic regions matrix and corresponding lookup tables are optional. A succession model table requires species regeneration probabilities.

The Base Fire model requires statistical fire distributions for fire regime regions, typically set to the biogeoclimatic region matrix. Base Fire requires parameters for the mean, minimum, and maximum event size, ignition probability (λ), and the mean fire rotation period for each of the fire regions. These parameters require adjustment to reproduce empirical fire distributions, typically achieved by manual approximation of the ignition probability and fire rotation period parameters (Syphard et al. 2007). To produce the desired fire regimes with high accuracy, we applied gradient descent for parameter optimization.

The Dynamic Fuels and Fire System (Dynamic Fire) model similarly requires fire regions, typically using the biogeoclimatic region matrix, and a corresponding lookup table. The model requires the expected mean (μ), standard deviation (σ), and maximum fire size for the log-normal distribution. The model also requires seasonal foliar moisture content (FMC) low and high averages, proportion of fires during high FMC conditions, open fuels class designation, and the annual frequency of fire initiation for each region. Dynamic Fire also requires a fire seasonality table containing leaf status, proportion of fires, percent curing, and fire-day-length-proportion parameters for each season. The model additionally requires a fuel-type table based on FBP System classes, which consists of parameters for base type, surface type, initiation probability, three fuel type-specific rate-of-spread constants, buildup index (BUI_S in the FBP System), maximum buildup effect (*q* in the FBP System), and crown base height, used to modify the initial spread index. The equations requiring these parameters have previously been described (Forestry Canada Fire Danger Group 1992; Finney 2002; Sturtevant et al. 2009).

The Dynamic Fire model's fire damage table requires parameters for the upper bound of the cohort age range and the minimum difference between fire severity and tolerance for mortality to occur. An initial weather database incorporating daily fire weather data, including fine fuel moisture code, buildup index, wind speed velocity, fire weather index, fire weather index bin, season, and ecoregion, is used to modify fuel conditions. To model the effects of topography on fire shape, users may input percent-slope and upslope-azimuth matrices, which we include using 90-meter NASA SRTM elevation data. The Dynamic Fire model requires a fuel coefficient for each species and a maximum-site-hardwood-percentage to be classified as a coniferous fuel group. The optional Dynamic Fuels submodel, which we include, requires a fuel type classification table in order to reclassify site fuel conditions following succession and/or disturbance. The table contains parameters for base fuel type, age range, and species presence/absence. A disturbance conversion table can optionally be used to allow other disturbance types to modify the site fuel classification (Sturtevant et al. 2009).

Model Parameterization

To parameterize the LANDIS-II model core, we used local species parameters derived from the literature and species compendiums (Burns and Honkala 1990; Farrar 1995). We applied Ward`s leptokurtic double-exponential seed dispersal algorithm within the succession model (Ward et al. 2004). To parameterize the initial landscape, we used a rules-based classification of species distributions for western North America (Gray and Hamann 2012). While bioclimatic envelope, or climate-equilibrium, models may not be suitable for forecasting under novel conditions, they can be used to accurately predict existing species distributions – a parameter difficult to estimate using remote sensing.

We classified modeled species frequency values into species cohorts using FBP System classes (Forestry Canada Fire Danger Group 1992). We binned forested sites into the following classes (FBP System code): Aspen (D-1); Boreal Spruce (C-2); Lodgepole or Jack Pine (C-3/C-4); Douglas-fir (C-7); Boreal Mixedwood (M-1/M-2). We set each site to even 0, 30, 60, and 90 year old age classes, relying on model spin-up to create historical forest structure patterns, given an absence of reliable forest age maps. For biogeoclimatic regions, we used a provincial classification scheme (Natural Regions Committee 2006).

We combined and reclassified Landcover for Agricultural Regions of Canada (Agriculture and Agri-Food Canada 2012) and Earth Observation for Sustainable Development of Forests (Wulder et al. 2007) data, each set to year 2000 conditions. We defined three base cell states: active-treed, active-untreed, and inactive. We classified the initial landscape to active-treed cells where species cohorts were present. We set herb, grassland, and shrubland landcover classes, to active-untreed, while setting agriculture, annual cropland, perennial crops and pasture, wetland, water, exposed land, snow/ice, rock/rubble, and built-up cells to inactive. Hence, forests and fires could expand into open natural areas given suitable conditions, but not into developed or resource-limited sites.

For Base Fire, we utilized historical fire data from the Canadian National Fire Database (Canadian Forest Service 2015) for 1923 to 2012, analyzed in a parallel study (Erickson et al., In Review). For the fire regions, we used the biogeoclimatic regions. We used the default fuel curve table to represent five fire severity classes, as it was created based on Canadian forests. We wrote R functions (R Core Team 2015) to calculate the mean, minimum, and maximum fire size, ignition probability, and fire rotation period for each fire region.

We developed a new parameter optimization technique for both fire models based on stochastic gradient descent (Widrow and Hoff 1960). First, coarse-resolution (500 m cell) simulations are run for the maximum duration (~1,000 years) to efficiently estimate the model signal for a given parameter space. Fire parameters for each region are then updated using the difference between actual and simulated values, before a new simulation begins. The process is repeated until the difference between actual and simulated fire regimes reaches a minimum. Specifically, the ignition probability is adjusted for each region until the simulated fire frequency is within 1% of the target range before the same optimization process is applied to *k* values, equivalent to the fire rotation period. We then computed final optimizations by running simulations at full resolution for the target duration, often producing little difference. Our fire parameter optimization method conceptually fuses sparse approximation with Monte Carlo signal processing methods and gradient descent. Our method reliably produced fire frequencies within 1% of the target values and area burned R^2 values over 0.99, compared to unoptimized values of 20% and 0.75, respectively. If fire regimes deviate significantly from a log-normal size distribution, Base Fire will be limited in its ability to reproduce them, but we did not experience that here.

For Dynamic Fire, we wrote R scripts (R Core Team 2015) to calculate the expected mean, standard deviation, maximum fire size, and annual fire frequency for each region and period. We wrote functions derived from the FBP System to calculate seasonal foliar moisture content (FMC) values. To do so, we calculated the regional minimum FMC date based on the mean latitude, longitude and elevation, before calculating the mid-season FMC using ordinal dates for the vernal equinox, summer solstice, autumnal equinox, and winter solstice. We used these values to calculate the proportion of fires occurring during the high FMC period. Low and high FMC thresholds were set to 25% and 75% of the maximum, respectively.

We used biogeoclimatic regions as the fire regions matrix. For percent ground slope and uphill azimuth, we used NASA SRTM3 version 2 data. For the fire seasons table, we set the leaf status for spring, summer, and fall to leaf-off, leaf-on, and leaf-off, respectively. We calculated the proportion of fires during each season by using a subset of the fire database, with dates converted to ordinal dates and seasons. The percent curing values were calculated as a function of FMC values, using a grassland curing index equation (Dilley et al. 2004), with the mean index value used to represent each season. Fire day length proportion was set to the standard value of one.

We calculated an initial fire weather database using Alberta Agriculture and Rural Development's historical fire weather station data. We selected fire weather stations with the shortest Euclidean distance to the centroid of each region. We used daily resolution fire weather data for the April 2012 through March 2013 fire weather season to represent recent climatic influences on fuels, as historical fire weather data is unavailable here. The weather metrics used include precipitation, mean temperature, mean humidity, wind speed at 10m above ground, and wind direction at 10m above ground. We used the R *mtsdi* package (Junger and de Leon 2012) to impute missing values for the period, using the default EM algorithm and splines method. We then used the R *fwi.fbp* package (Wang et al. 2014) to calculate daily fine fuel moisture content, build-up index, and fire weather index using standard equations (Van Wagner 1987). We segmented fire weather index values into five bins based on quantile groups using the R *Hmisc* package (Harrell and Dupont 2015).

To parameterize the fuel type table, we used FBP System fuel classes and parameters developed for Canada (Forestry Canada Fire Danger Group 1992). These parameters include base type, surface type, initiation probability, *a*, *b*, and *c* rate-of-spread parameters, a *q* depth dryness parameter, build-up index, maximum build-up effect, and crown base height. We set the fuel types not currently present in the landscape to inactive. We used a standard fire damage table, with probability of mortality inversely related to cohort age. The table includes species-specific fire tolerances, with standard transitions at 20%, 50%, 85% and 100% age percent of longevity.

We used the optional dynamic fuels submodel, reclassifying site fuel conditions at the end of each simulation year. This enables fire behavior to more realistically respond to succession and disturbance. To parameterize the fuels model, we assigned species an even fuel reclassification weighting coefficient of 1.0. We set deciduous species maximum composition for conifer stands to the standard 10%. We based the fuel type reclassification table on the FBP System, utilizing its definitions for species composition and age classes (Forestry Canada Fire Danger Group 1992).

Tree species life history attributes for LANDIS-II (Supplementary material, Table S3) were derived from the following sources: balsam fir *(Abies balsamea)* (Xu et al. 2010); subalpine fir (*Abies lasiocarpa*) (Burns and Honkala 1990; Farrar 1995); paper birch (*Betula papyrifera*) (Peterson et al. 1997; Government of Alberta 2009); larch (*Larix laricina*) (Burns and Honkala 1990; Farrar 1995); western larch (*Larix occidentalis*) (Burns and Honkala 1990); Engelmann spruce (*Picea engelmannii*) (McCune and Allen 1985; Burns and Honkala 1990; Government of Alberta 2009); white spruce (*Picea glauca*) (Dobbs 1976; Groot et al. 2003; Government of Alberta 2009); black spruce (*Picea mariana*) (Stanek 1961; Burns and Honkala 1990;

Government of Alberta 2009); jack pine (*Pinus banksiana*) (Flannigan and Wotton 1994; Farrar 1995; Government of Alberta 2009); lodgepole pine (*Pinus contorta*) (Lotan and Perry 1983; Parminter 1984; Burns and Honkala 1990; Farrar 1995); western white pine *(Pinus monticola)* (Burns and Honkala 1990; Owens and Bruns 2000; Organisation for Economic Co-operation and Development 2006);; balsam popular (*Populus balsamifera*) (Burns and Honkala 1990; Farrar 1995); trembling aspen (*Populus tremuloides*) (DeByle and Winokur 1985; Burns and Honkala 1990; Jelinski et al. 1992; Huang et al. 1992; United States Forest Service 2013).

Gradient-based Optimization

Generally, gradient-based strategies search for a minimum to a *D*-dimensional target (also objective or cost) function $f(\vec{x})$ approximated by a terminated Taylor series expansion around $\vec{x}_0$:

$$f(\vec{x}_0+\vec{x}) \approx f(\vec{x}_0)+\left(\nabla f(\vec{x}_0)\right)^T \vec{x}+\frac{1}{2}\vec{x}^T \nabla^2 f(\vec{x}_0)\vec{x}$$

Optimization is performed iteratively by beginning at an initial value $x_{i=0}$ and computing its target function $f(\vec{x}_i)$value, before searching for a minimum in the following loop:

1. Check for convergence of $f(\vec{x}_i)$ per a given criterion; if fulfilled, accept $\vec{x}_i$
2. Compute the gradient direction $\vec{p}_i$ and step width or learning rate l_i
3. Evaluate the new point in the parameter space $\vec{x}_{i+1}=\vec{x}_i+\vec{p}_i \cdot l_i$; compute the target $f(\vec{x}|i+1)$ and return to step 1

A first-order linear approximation can be used to compute the step direction p_i of the target function:

$$f\left(\vec{x}_0+\vec{p}\right)\approx f\left(\vec{x}_0\right)+\left(\nabla f\left(\vec{x}_0\right)\right)^T\vec{p}$$

This results in the following step direction p_i, known as the steepest descent method:

$$\vec{p}=-\nabla f\left(\vec{x}_0\right)$$

The gradient vector is orthogonal to the plane tangent to the isosurfaces of the function $f\left(\vec{x}\right)$. Gradient descent adds stochasticity to the optimization process in order to improve search space coverage and convergence toward a global minimum, avoiding local minima or saddle points. The standard gradient descent algorithm updates the parameters $\vec{x}$ of target function $f\left(\vec{x}\right)$:

$$\vec{x}=\vec{x}-l\nabla_x E\left(f\left(\vec{x}\right)\right)$$

The expectation E is calculated by evaluating the gradient over the entire training dataset. Stochastic gradient descent removes the expectation in the update and instead computes the gradient of parameters using one to few training samples.

The SGD update is as follows:

$$\vec{x}=\vec{x}-l\nabla_x f\left(\vec{x};x_i,y_i\right)$$

Tables

Table S1. Simulation scenario codes based on model configuration and period

LANDIS-II Configuration	Period	Abbreviation
Age-only succession	1923-1952	ao-1923-1952
Age-only succession	1953-1982	ao-1953-1982
Age-only succession	1983-2012	ao-1983-2012
Age-only succession	2003-2012	ao-2003-2012
Age-only succession with base fire	1923-1952	ao-bf-1923-1952
Age-only succession with base fire	1953-1982	ao-bf-1953-1982
Age-only succession with base fire	1983-2012	ao-bf-1983-2012
Age-only succession with base fire	2003-2012	ao-bf-2003-2012
Age-only succession with dynamic fire	1923-1952	ao-dffs-1923-1952
Age-only succession with dynamic fire	1953-1982	ao-dffs-1953-1982
Age-only succession with dynamic fire	1983-2012	ao-dffs-1983-2012
Age-only succession with dynamic fire	2003-2012	ao-dffs-2003-2012
Age-only succession with base fire	Extremes	ao-bf-extremes
Age-only succession with dynamic fire	Extremes	ao-dffs-extremes

Table S2. Soils parameters used in TACA-EM

Natural Subregion	Soil Texture	Rooting Zone Depth (m)	Coarse Fragment %	AWSC (mm/m)	Field Capacity (mm/m)	Percolation (mm/day)	Latitude
Alpine	-	-	-	-	-	-	-
Central Mixedwood	SiCL	1.0	5%	452	560	93.1	55°
Central Parkland	CL	1.0	5%	341	470	122.6	50°
Dry Mixedwood	CL	1.0	5%	341	470	122.6	55°
Foothills Fescue	CL	1.0	5%	341	470	122.6	50°
Foothills Parkland	CL	1.0	20%	341	470	103.2	50°
Lower Boreal Highlands	CL	1.0	20%	341	470	103.2	55°
Lower Foothills	CL	1.0	5%	341	470	122.6	55°
Mixedgrass	CL	1.0	5%	341	470	122.6	50°
Montane	L	1.0	20%	377	460	66.4	50°
Peace River Parkland	CL	1.0	5%	341	470	122.6	55°
Subalpine	L	1.0	20%	377	460	66.4	50°
Upper Boreal Highlands	CL	1.0	20%	341	470	103.2	55°
Upper Foothills	CL	1.0	5%	341	470	122.6	55°

Table S3. Tree species biophysical parameters used in TACA-EM

Species	Model Code	Physiological Base Temperature (°C)	Heat Sum for Bud Burst (GDD)	Chilling Requirement (Days)	Minimum Temperature (°C)	Drought Tolerance	GDD Minimum	GDD Maximum	Frost Tolerance	Frost Season	Wet Soils	Heat Moisture Index
Abies balsamea	Sp1	2.8	121	49	-62	0.20	560.0	2,386	0.9	305	0.55	41.4
Abies lasiocarpa	Sp3	2.6	119	70	-67	0.25	197.6	5,444	0.9	320	0.75	28.7
Betula payrifera	Sp5	3.7	231	77	-80	0.30	236.8	4,122	0.9	285	0.30	40.0
Larix laricina	Sp7	2.9	111	42	-76	0.20	150.8	3,331	0.9	300	0.75	33.8
Larix occidentalis	Sp8	3.4	180	70	-40	0.40	163.2	3,057	0.7	305	0.05	38.7
Picea engelmannii	Sp9	3.1	145	49	-64	0.25	74.4	2,150	0.9	335	0.50	28.7
Picea glauca	Sp10	2.7	147	42	-69	0.34	129.6	3,459	0.9	305	0.50	43.2
Picea mariana	Sp11	3.0	123	56	-69	0.30	144.0	3,060	0.9	305	1.00	42.7
Pinus banksiana	Sp13	2.8	108	56	-85	0.50	830.0	2,216	0.9	320	0.30	37.9
Pinus contorta	Sp14	2.9	116	63	-85	0.42	185.6	3,374	0.9	320	0.50	37.9
Pinus monticola	Sp15	4.4	468	98	-85	0.25	211.2	3,554	0.75	305	0.50	25.8
Populus balsamifera	Sp17	2.1	93	49	-80	0.13	126.0	7,852	0.9	290	0.55	59.0
Populus tremuloides	Sp18	3.5	189	70	-80	0.40	226.8	4,414	0.9	284	0.30	40.0

Table S4. Tree species life history attribute parameters used in LANDIS-II

Species	Longevity	Sexual Maturity Age	Shade Tolerance	Fire Tolerance	Effective Seed Dispersal Distance	Maximum Seed Dispersal Distance	Vegetative Reproduction Probability	Sprouting Minimum Age	Sprouting Maximum Age	Post-Fire Regeneration
Abies balsamea	150	25	5	1	30	160	-1	-1	-1	None
Abies lasiocarpa	200	20	4	2	30	80	0.05	20	200	None
Betula papyrifera	150	15	2	1	100	200	0.5	1	60	Resprout
Larix laricina	150	10	1	3	38	60	0.05	10	150	None
Larix occidentalis	400	15	1	5	100	240	-1	-1	-1	None
Picea engelmannii	720	15	3	2	46	183	0.05	15	720	None
Picea glauca	350	25	3	2	100	300	0.05	25	350	None
Picea mariana	150	30	4	1	260	260	0.05	30	200	Serotiny
Pinus banksiana	200	10	2	4	37	60	-1	-1	-1	Serotiny
Pinus contorta	200	5	2	4	27	200	-1	-1	-1	Serotiny
Pinus monticola	350	7	3	3	120	800	-1	-1	-1	None
Populus balsamifera	200	9	2	3	50	3000	0.5	9	200	Resprout
Populus tremuloides	200	2	1	4	uni	5000	0.95	1	200	Resprout

Table S5. Fire regime statistics by period for the study area

Period	Burned (ha)	Area (ha)	FRP	MFRI	MFS
1923-1952	3,224,691	24,972,634	232.326	0.011	1,148.394
1953-1982	1,211,806	24,972,634	618.234	0.020	811.115
1983-2012	809,967	24,972,634	924.950	0.020	545.066
2003-2012	270,287	24,972,634	923.931	0.011	308.899

Table S6. Simulated and observed fire time-series statistics; WD = wavelet dissimilarity

Period	Simulation	Mean$_{area}$	SD$_{area}$	r_{area}	WD$_{area}$	Mean$_{freq.}$	SD$_{freq.}$	$r_{freq.}$	WD$_{freq.}$
1923-1952	Base Fire	+70,282	+375,027	-0.10	49.594	+696.8	+82.9	0.42	46.976
1923-1952	Dynamic Fire	-18,385	-168,825	-0.14	48.496	+54.3	-8.8	0.05	39.841
1953-1982	Base Fire	-27,265	-66,458	0.25	46.235	+357.6	+17.5	-0.29	42.179
1953-1982	Dynamic Fire	-3,338	-59,027	0.07	48.456	+39.9	-2.7	0.11	40.394
1983-2012	Base Fire	-20,689	-51,047	0.21	47.059	+202.3	-5.7	0.68	38.613
1983-2012	Dynamic Fire	-1,529	-46,255	-0.02	47.939	+55.4	-14.9	0.17	36.923
2003-2012	Base Fire	-18,363	-40,783	-0.06	15.150	+352.4	-4.6	0.07	14.528
2003-2012	Dynamic Fire	-5,121	-31,994	-0.58	15.377	+152.6	+42.8	0.13	14.360

1181 **Figures**

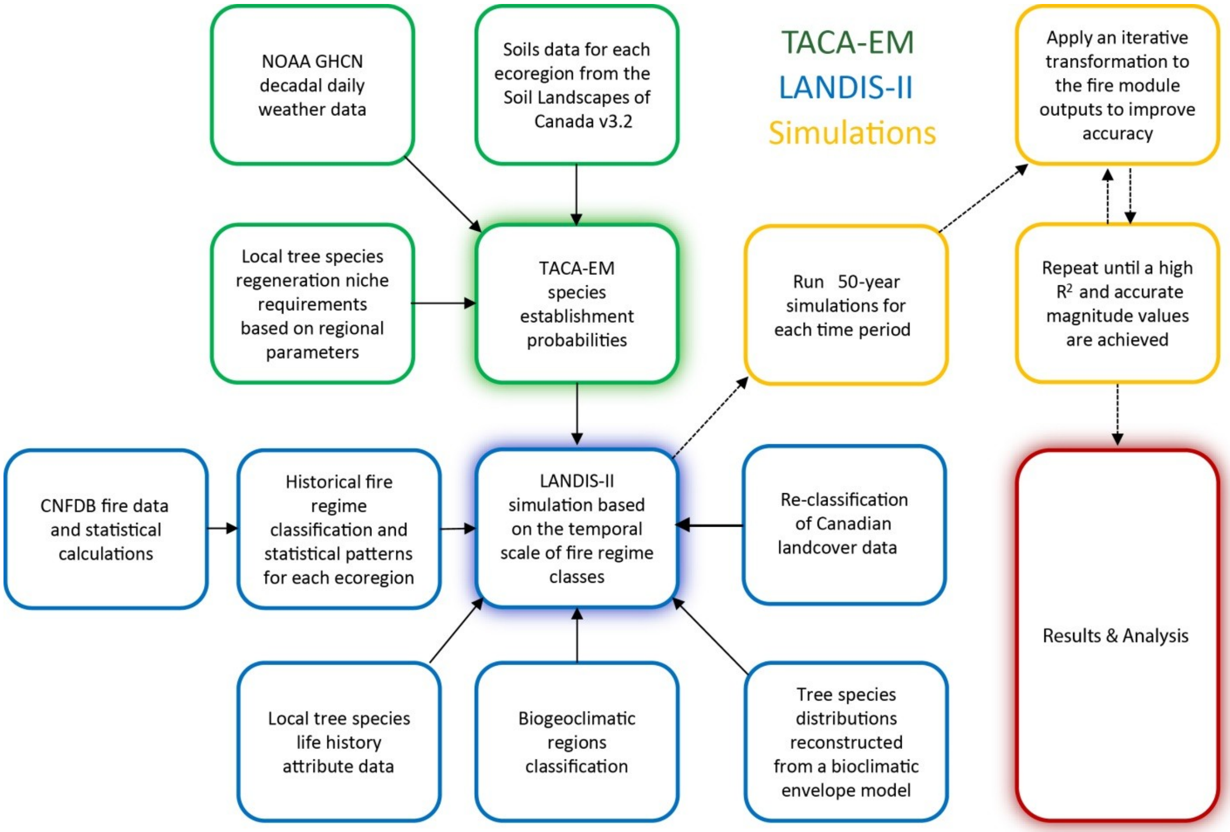

1182

1183 Figure S1. Overall simulation framework used in this study

1184

1185

1186

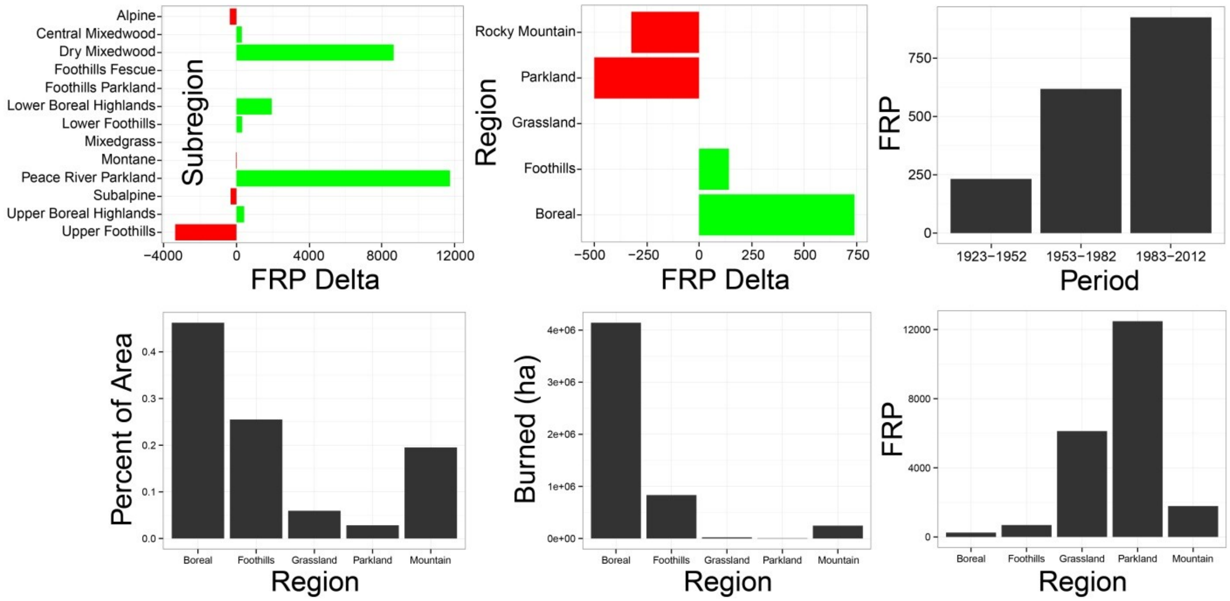

Figure S2. Historical fire statistics by region and time period; change metrics are computed between the periods 1923-1952 and 1983-2012: (top-left) Fire rotation period (FRP) change by subregion; (top-middle) FRP change by region; (top-right) FRP by period; (bottom-left) fraction of area burned by region; (bottom-middle) total area burned by region; (bottom-right) FRP by region; Montane region = Rocky Mountain; red = decline; green = increase

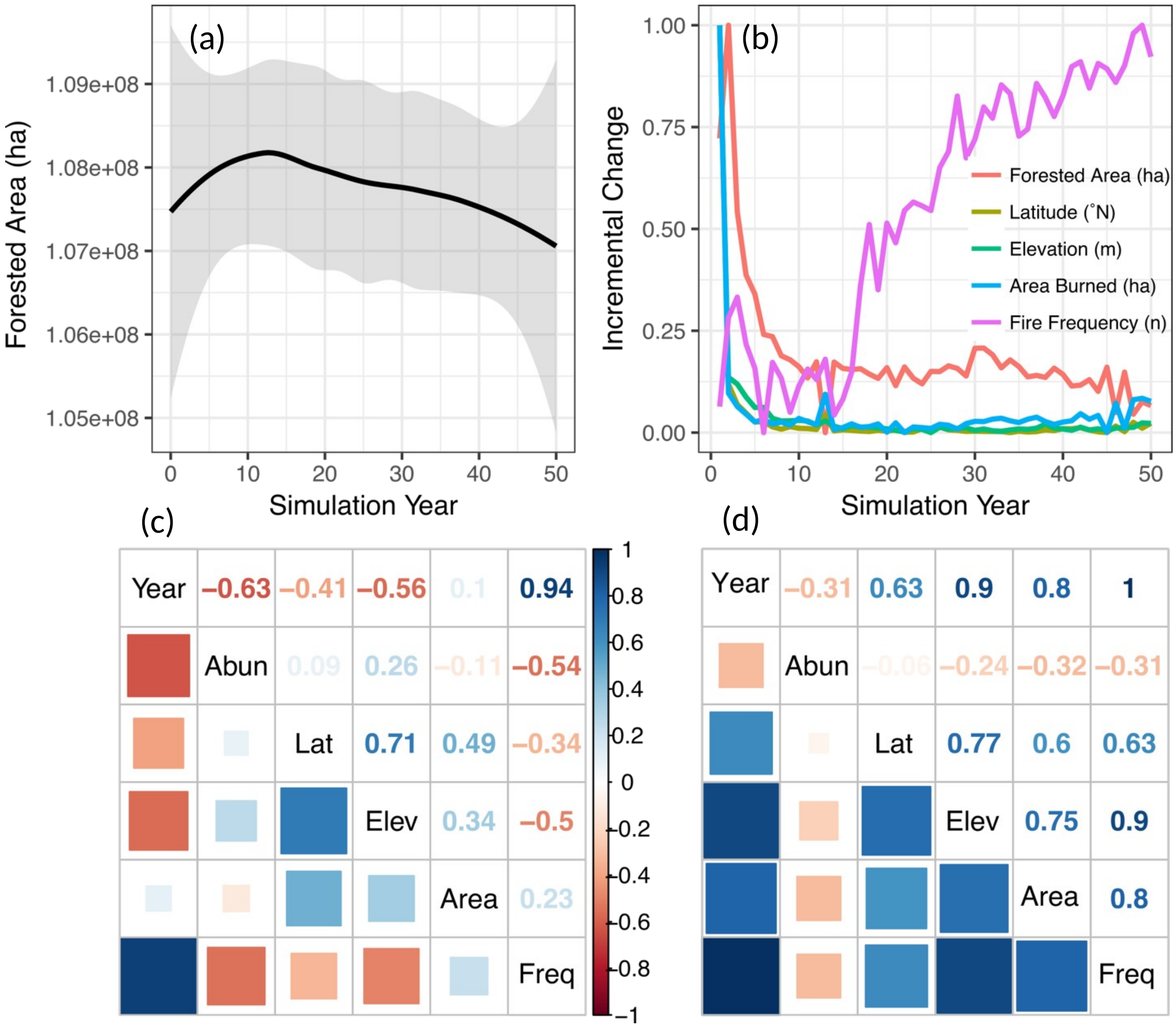

Figure S3. Mean annual simulated forest change: (a) total forested area for all scenarios with a 95% confidence interval; (b) re-scaled forested area, latitude, elevation, area burned, and fire frequency for all scenarios; (c) Spearman's ρ for re-scaled metrics; (d) Spearman's ρ for autocorrelations of re-scaled metrics; Abun = forest area; Lat = forest latitude; Elev = forest elevation; Area = area burned; Freq = fire frequency

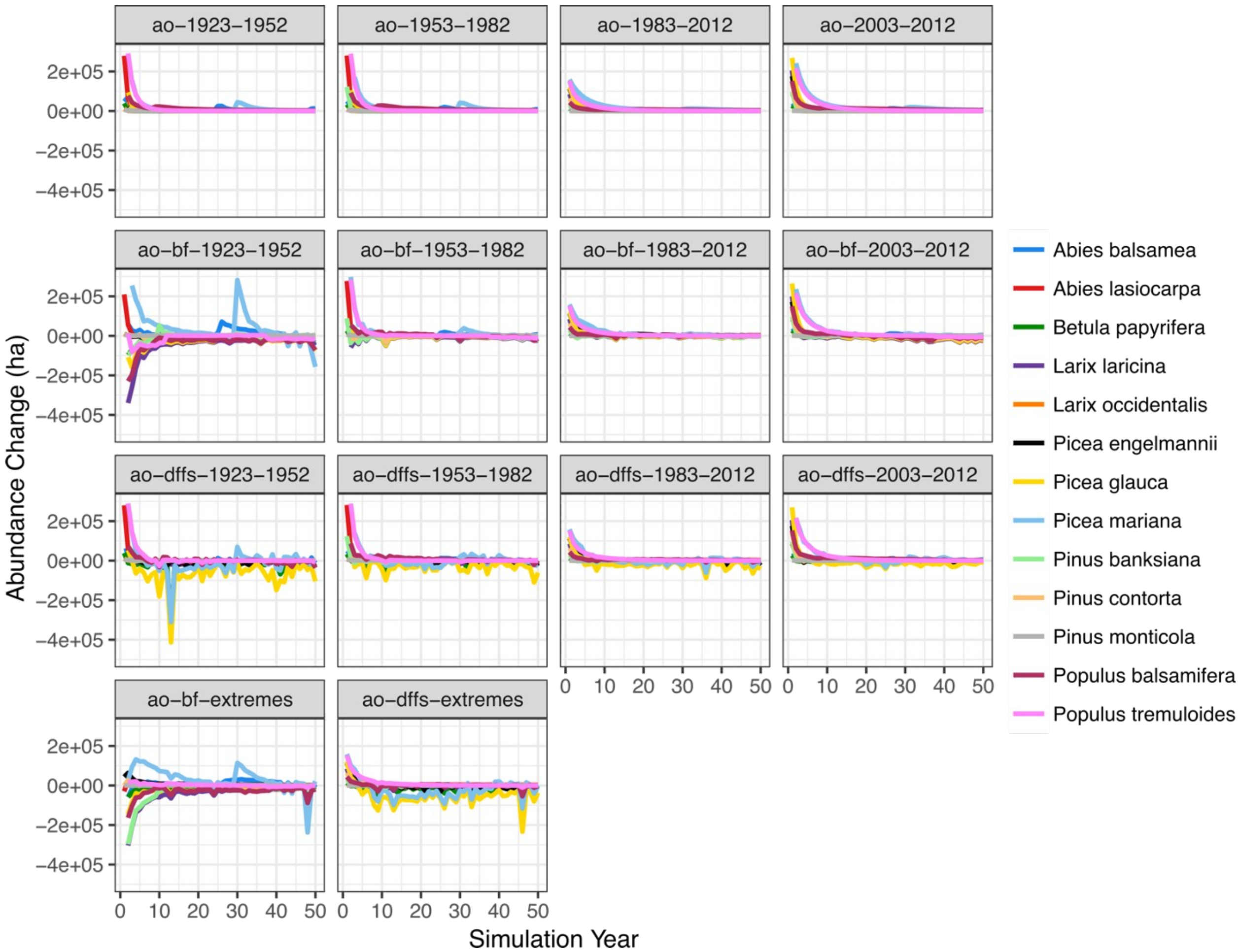

Figure S4. Simulated annual incremental change in species abundance by scenario; refer to Table S1 for scenario codes